Attachment 2

Non-Proprietary Version
WCAP-14770, Structural Integrity Evaluation of Reactor Vessel Upper Head Penetrations to Support Continued Safe Operation of North Anna and Surry Units
Revision 0

North Anna Power Station Unit 2
Virginia Electric and Power Company
(Dominion)

Westinghouse Non-Proprietary Class 3

WCAP - 15770
Revision 0

Structural Integrity Evaluation of Reactor Vessel Upper Head Penetrations to Support Continued Operation: North Anna and Surry Units

Westinghouse Electric Company LLC

WCAP-15770

Structural Integrity Evaluation of Reactor Vessel Upper Head Penetrations to Support Continued Operation: North Anna And Surry Units

W. H. Bamford
J. F. Duran
K. R. Hsu

November 2001

Reviewed by: P. L. Strauch

Approved by: S. A. Swamy, Manager
Structural Mechanics Technology

Westinghouse Electric Company LLC
P.O. Box 355
Pittsburgh, PA 15230-0355

©2001 Westinghouse Electric Company LLC

5779.wpd(111901)

TABLE OF CONTENTS

		Page No.
1.0	INTRODUCTION	1-1
2.0	HISTORY OF CRACKING IN HEAD PENETRATIONS	2-1
3.0	OVERALL TECHNICAL APPROACH	3-1
	3.1 Penetration Stress Analysis	3-1
	3.2 Flaw Tolerance Approach	3-2
4.0	MATERIAL PROPERTIES, FABRICATION HISTORY, AND CRACK GROWTH PREDICTION	4-1
	4.1 Materials and Fabrication	4-1
	4.2 Crack Growth Prediction	4-1
5.0	STRESS ANALYSIS	5-1
	5.1 Objectives of the Analysis	5-1
	5.2 Model	5-1
	5.3 Stress Analysis Results - Outermost Penetration	5-1
	5.4 Stress Analysis Results - Next Outermost Penetration	5-2
	5.5 Stress Analysis Results - Center Penetration	5-3
6.0	FLAW EVALUATION CHARTS	6-1
	6.1 Introduction	6-1
	6.2 Overall Approach	6-3
	6.3 Results: Axial Flaws	6-3
	6.4 Circumferential Crack Propagation	6-4
	6.5 Flaw Acceptance Criteria	6-7
7.0	FLAW DISPOSITION STRATEGIES	7-1
	7.1 Axial Flaws in the Penetration Tube At and Above Weld	7-2
	7.2 Axial Flaws in the Penetration Tube Below the Weld	7-2
	7.3 Flaws in the Attachment Weld	7-3
	7.4 Circumferential Flaws Above the Attachment Weld	7-3
8.0	SUMMARY AND CONCLUSIONS	8-1

TABLE OF CONTENTS (cont)

	Page No.
9.0 REFERENCES	9-1
APPENDIX A: Allowable Areas of Lack of Fusion: Weld Fusion Zones	A-1
APPENDIX B: Example Calculations	B-1

SECTION 1.0
INTRODUCTION

In September of 1991, a leak was discovered in the reactor vessel control rod drive head penetration region of an operating plant. The geometry of interest is shown in Figure 1-1.

The leak resulted from cracking which occurred in the outermost penetration. Similar cracking occurred at a number of operating plants, as discussed in Section 2. This outermost penetration, the next outermost and the center penetration, were chosen for fracture mechanics analyses to support continued safe operation of the North Anna and Surry Units, if such cracking were to be found. The head penetration geometries of these four units are nearly identical, so a single set of analyses was performed to bound all four units.

The basis of the analyses was a detailed three dimensional elastic-plastic finite element analysis of the penetration locations, as described in detail in Section 5. The geometry of the outermost "hillside" penetrations analyzed is shown in Figure 1-2.

The fracture analyses used reference crack growth rates developed from the literature and from service experience. The results are presented in the form of flaw evaluation charts in Section 6, for both surface and through wall flaws, to determine the allowable time of safe operation if indications are found. All the times calculated in this handbook are effective full power years.

<u>Revision 1</u> This revision was prepared to incorporate editorial corrections in Table 2-1 and Figure 6-1. The discussion of flaw disposition strategies in Section 7 has been revised to be more complete and to reference the NRC concurrence with the embedded flaw repair strategy. Also the development of the crack growth law in Section 4.2 has been revised to provide more detail.

<u>Revision 2</u> This revision was prepared to update the inspection experience through the spring of 2001, and to include newly prepared flaw evaluation charts for flaws originating on the outside surface of the penetrations. Also the circumferential flaw evaluation charts were revised to be more accurate and to provide a more complete basis for their construction.

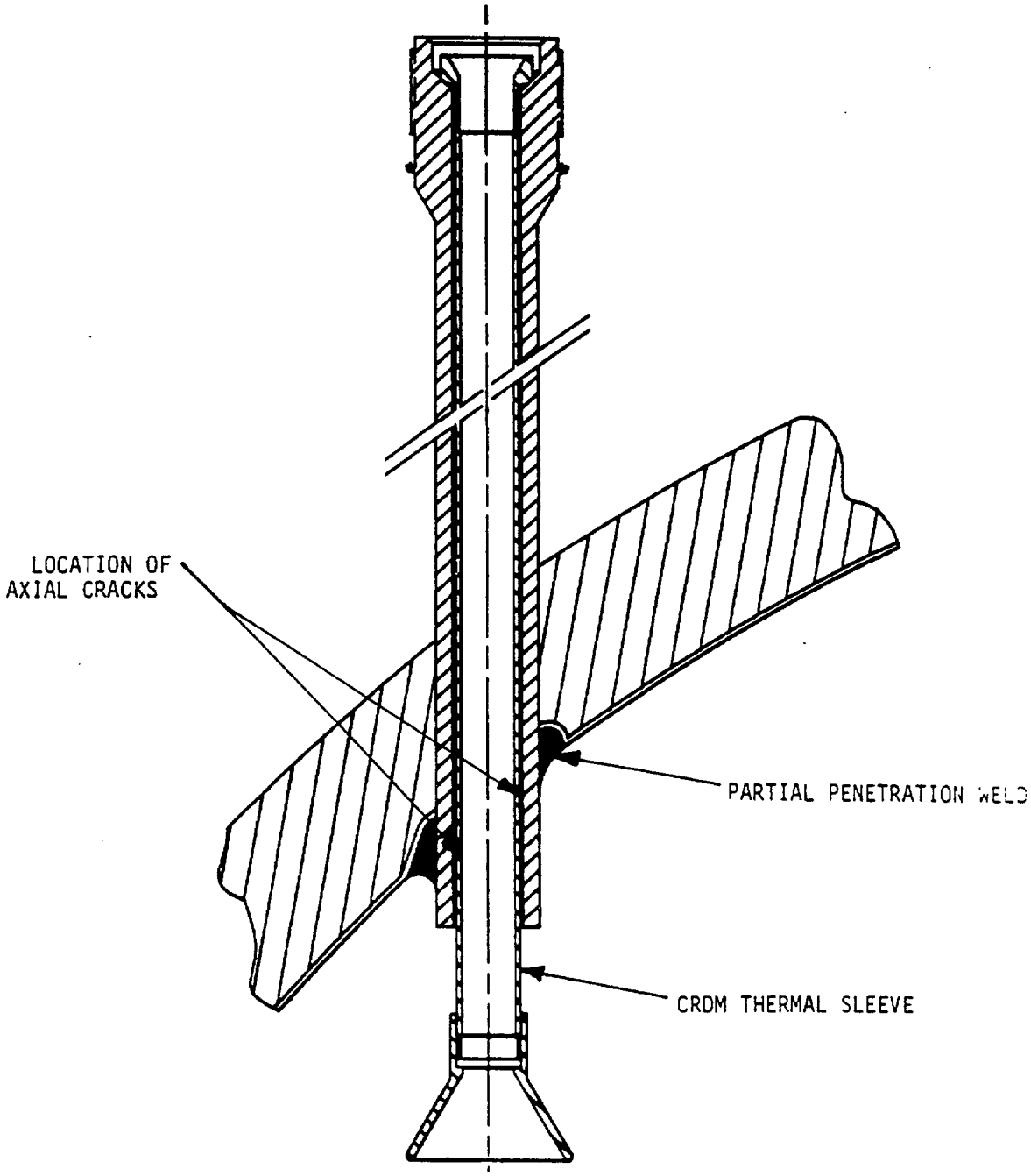

FIGURE 1-1

REACTOR VESSEL HEAD ADAPTER PENETRATION TUBE, SHOWING LOCATIONS OF AXIAL CRACKS FOUND IN SOME PLANTS

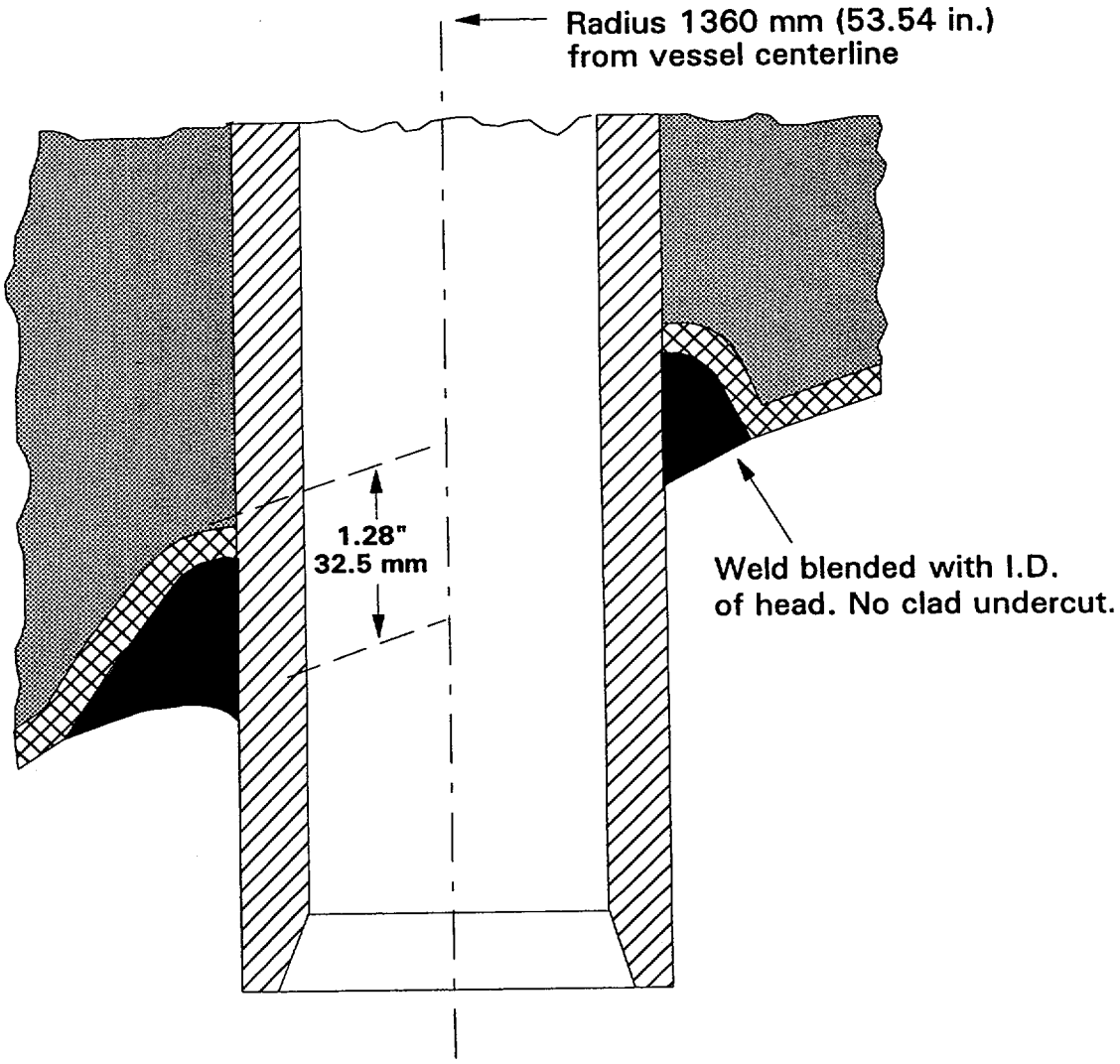

FIGURE 1-2

GEOMETRY OF THE HILLSIDE PENETRATIONS ANALYZED

SECTION 2.0
HISTORY OF CRACKING IN HEAD PENETRATIONS

In September of 1991, leakage was reported from the reactor vessel head penetration region of a French plant, Bugey Unit 3. Bugey 3 is a 920 megawatt three-loop PWR which had just completed its tenth fuel cycle. The leak occurred during a post ten year hydrotest conducted at a pressure of approximately 3000 psi (204 bar) and a temperature of 194°F (90°C). The leak was detected by metal microphones located on the top and bottom heads, and the leak rate was estimated to be approximately 0.7 liter/hour. The location of the leak was at a peripheral penetration with an active control rod (H-14), as seen in Figure 2-1.

The control rod drive mechanism (CRDM) and thermal sleeve were removed from this location to allow further examination. Further study of the head penetration revealed the presence of longitudinal cracks near the head penetration attachment weld. Penetrant and ultrasonic testing confirmed the cracks. The cracked penetration was fabricated from Alloy 600 bar stock (SB-166), and has an outside diameter of 4 inches (10.16 cm) and an inside diameter of 2.75 inches (7.0 cm).

As a result of this finding, all of the control rod drive mechanisms and thermal sleeves at Bugey 3 were removed for inspection of the head penetrations. Only two penetrations were found to be cracked, as shown in Figure 2-1.

An inspection of a sample of penetrations at three additional plants were planned and conducted during the winter of 1991-92. These plants were Bugey 4 , Fessenheim 1, and Paluel 3. The three outermost rows of penetrations at each of these plants were examined, and further cracking was found in two of the three plants.

At Bugey 4, eight of the 64 penetrations examined were found to contain axial cracks, while only one of the 26 penetrations examined at Fessenheim 1 was cracked. The locations of all the cracked penetrations are shown in Figure 2-1. None of the 17 penetrations inspected at Paluel 3 showed indications of cracking at the time. Further inspections of all French plants have confirmed cracking in nearly all of them. The cracking found to date has been consistent in both location and extent. All cracks discovered by nondestructive examination have been oriented axially, and have been located in the bottom portion of the penetration in the vicinity of the partial penetration attachment weld to the vessel head as shown schematically in Figure 1-1.

[

]a,c,e

Non-destructive examinations of the leaking CRDM nozzles showed that most of the cracks originated on the outside surface of the nozzles below the J-groove weld, were axially oriented, and propagated primarily in the nozzle base material to an elevation above the top of the J-groove weld where leakage could then pass through the annulus to the top of the head where it was detected by visual inspection. In some cases the cracks initiated in the weld metal or propagated into the weld metal, and in a few cases the cracks propagated through the nozzle wall thickness to the inside surface.

[

]a,c,e

[

]a,c,e

The cracking has now been confirmed to be primary water stress corrosion cracking (PWSCC). Relatively high residual stresses are produced in the outermost penetrations due to the welding process. Other important factors which affect this process are temperature and time, with higher temperatures and longer times being more detrimental. The inspection findings for the plants examined thus far are summarized in Table 2-1.

While the inspection findings in Table 2-1 are very interesting, revealing that only 4.8 percent of the 6005 penetrations inspected have been cracked, the table presents no information about the location of the indications. Figure 2-1 shows that most of the indications have been found in the outer three rows of the penetrations, regardless of the plant design. It should be noted that the recent leaks at Oconee and ANO were distributed randomly throughout the head. The location of these indications relative to the attachment weld, and relative to the circumference of the penetration is not provided. Figure 2-2 provides a summary of the indications discovered in French plants, plotted as a function of the azimuthal location. Both the upper and lower extremities of the flaws are plotted, as a function of the distance from the bottom of the penetration (denoted as elevation).

It is interesting to note that the majority of flaws are clustered at the 180 degree azimuth location (nearest the vessel center) and at zero degrees (furthest from the vessel center). In addition, the uppermost extent of the flaws has been at about the same elevation (140 mm) regardless of the angular location. There are three exceptions to this trend, but they occurred at the Bugey 3 Plant, which is where the through-wall leak occurred. This is an acknowledged outlier.

It may be deduced from the data that flaws are not expected near the weld on the center side

(180° location) of the penetrations. This is a favorable conclusion, since there is a spacer bar on the North Anna thermal sleeves at this level which significantly restricts inspection above the weld for penetrations with thermal sleeves. The table below shows that the spacer is considerably higher than the 140 mm level for the North Anna penetrations.

a,c,e

TABLE 2-1
OPERATIONAL INFORMATION AND INSPECTION RESULTS FOR UNITS EXAMINED
(RESULTS TO APRIL 30, 2001)

Country	Plant Type	Units Inspected	K Hours	Head Temp. (°F)	Total Penetrations	Penetrations Inspected	Penetrations With Indications
France	CPO	6	80-107	596-599	390	390	23
	CPY	28	42-97	552	1820	1820	126
	1300MW	20	32-51	558-597	1542	1542	95
Sweden	3 Loop	3	75-115	580-606	195	190	8
Switzerland	2 Loop	2	148-154	575	72	72	2
Japan	2 Loop	7	105-108	590-599	276	243	0
	3 Loop	7	99	610	455	398	0
	4 Loop	3	46	590	229	193	0
Belgium	2 Loop	2	115	588	98	98	0
	3 Loop	5	60-120	554-603	337	337	6
Spain	3 Loop	5	65-70	610	325	102	0
Brazil	2 Loop	1	25	NA	40	40	0
South Africa	3 Loop	1	NA	NA	65	65	6
Slovenia	2 Loop	1	NA	NA	49	49	0
South Korea	2 Loop	3	NA	NA	49	49	3
	3 Loop	2	NA	NA	130	130	2
US	2 Loop	2	170	590	98	98	0
	3 Loop	1	NA	NA	65	20	0
	4 Loop	7	NA	NA	221	169	16
TOTALS		103	–	–	6456	6005	287

FRENCH R/V CLOSURE HEAD PENETRATION CRACKING
EdF PLANTS - PENETRATIONS WITH CRACKING

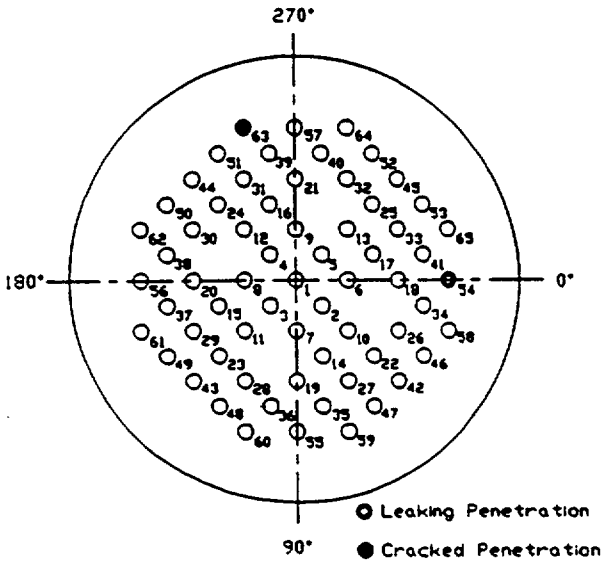

BUGEY 3

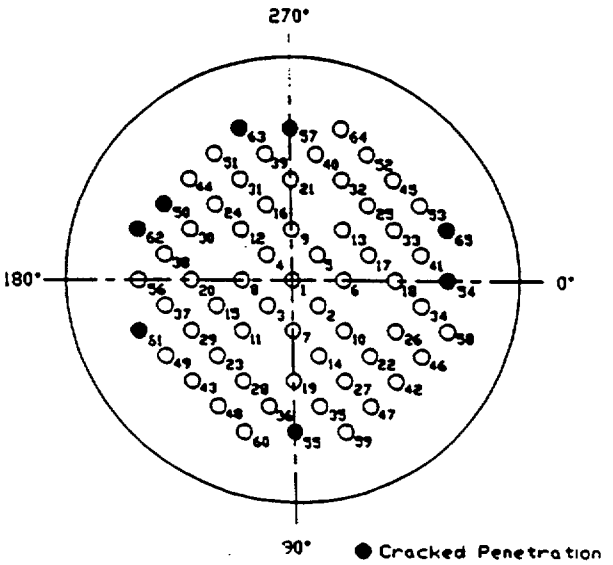

BUGEY 4

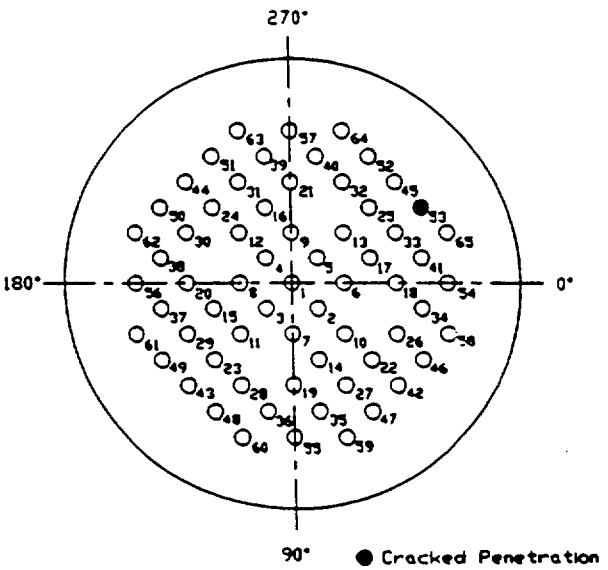

FESSENHEIM 1

FIGURE 2-1

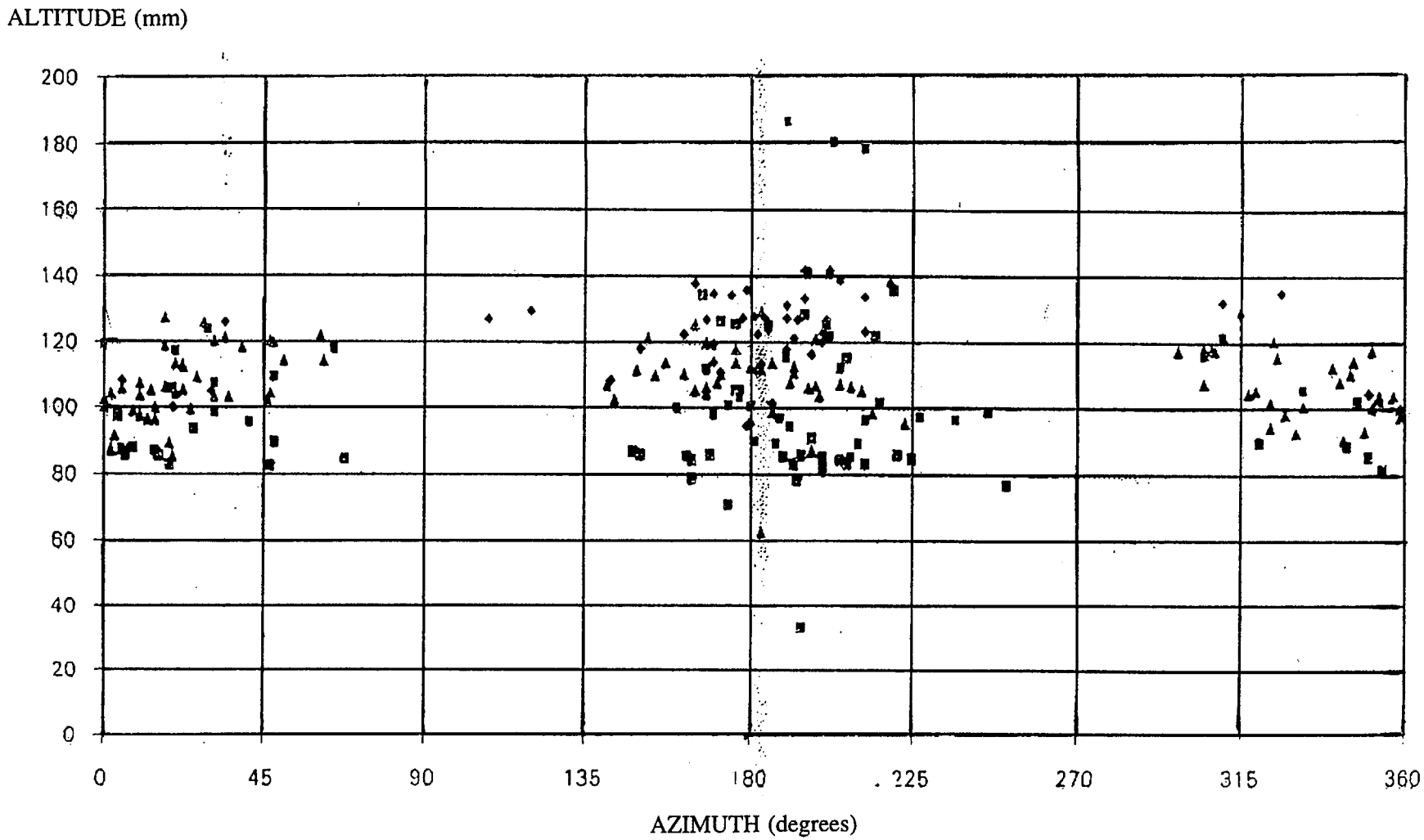

FIGURE 2-2
SUMMARY OF INDICATIONS IN FRENCH PLANTS AS A FUNCTION OF ANGULAR AZIMUTH AND HEIGHT

SECTION 3.0
OVERALL TECHNICAL APPROACH

The primary goal of this work is to provide technical justification for the continued safe operation of the North Anna and Surry Units in the event that cracking is discovered during inservice inspections of the Alloy 600 reactor vessel head penetrations.

3.1 PENETRATION STRESS ANALYSIS

[

]a,c,e

Three dimensional elastic-plastic finite element stress analyses have been performed to determine the stresses in the head penetration region. These analyses have considered the pressure and thermal transient loads associated with steady state operation, as well as the residual stresses which are produced by the fabrication process.

[ ]a,c,e

3.2 FLAW TOLERANCE APPROACH

A flaw tolerance approach has been developed to allow continued safe operation until an appropriate time for repair, or the end of plant life. The approach is based on the prediction of future growth of detected flaws, to ensure that such flaws would remain stable.

If an indication is discovered during inservice inspection, its size can be compared with the flaw size which is considered allowable for continued service. This "allowable" flaw size is determined from the acceptance criteria proposed by industry and accepted by the NRC. Suitable margins to ensure the integrity of the reactor vessel as well as safety from unacceptable leakage rates, have been considered. Acceptance criteria are discussed in Section 6.5.

The time for the observed crack to reach the allowable crack size determines the length of time the plant can remain online before repair, if required.

The results of the evaluation are presented in terms of simple charts, which show graphically the time required to reach the allowable size, which represents the additional service life before repair. This result is a function of the loadings on the particular head penetration, the initial crack size, and the circumferential location of the crack in the penetration tube.

Schematic drawings of the head penetration flaw tolerance charts are presented as Figures 3-1 and 3-2. These two types of charts can be used to provide estimates of the time which remains before a leak would develop from an observed crack. For example, if a part-through flaw was discovered, the user would first refer to Figure 3-1, to determine the time (t_P) which would be remaining before the crack would penetrate the wall or reach the allowable depth (eg a/t=.75). Once the crack penetrates the wall, the time (t_B) required to reach an allowable crack length would be determined from Figure 3-2. The allowable crack depth or length is a function of the crack location, and is defined in the industry acceptance criteria discussed in Section 6.5. The total time remaining would then be the simple sum:

$$\text{Time remaining} = t_P + t_B$$

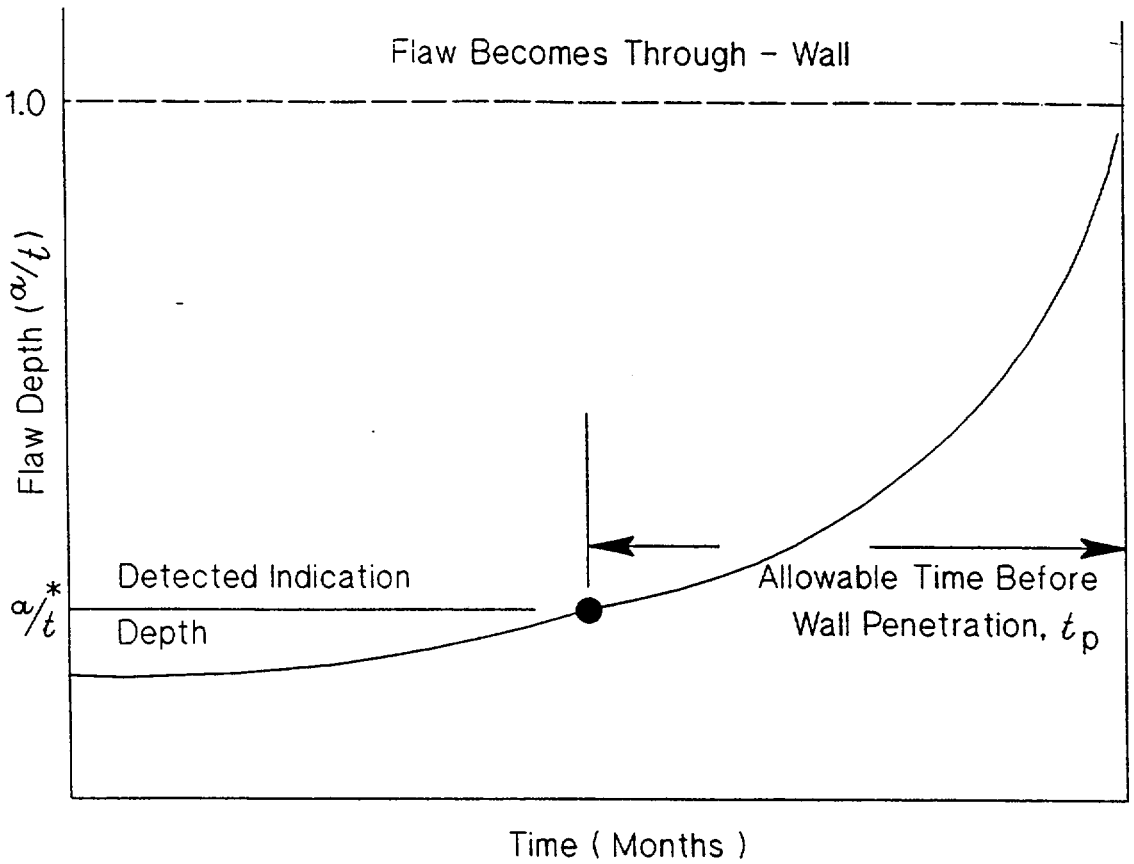

FIGURE 3-1

SCHEMATIC OF A HEAD PENETRATION FLAW GROWTH CHART

FOR PART THROUGH FLAWS

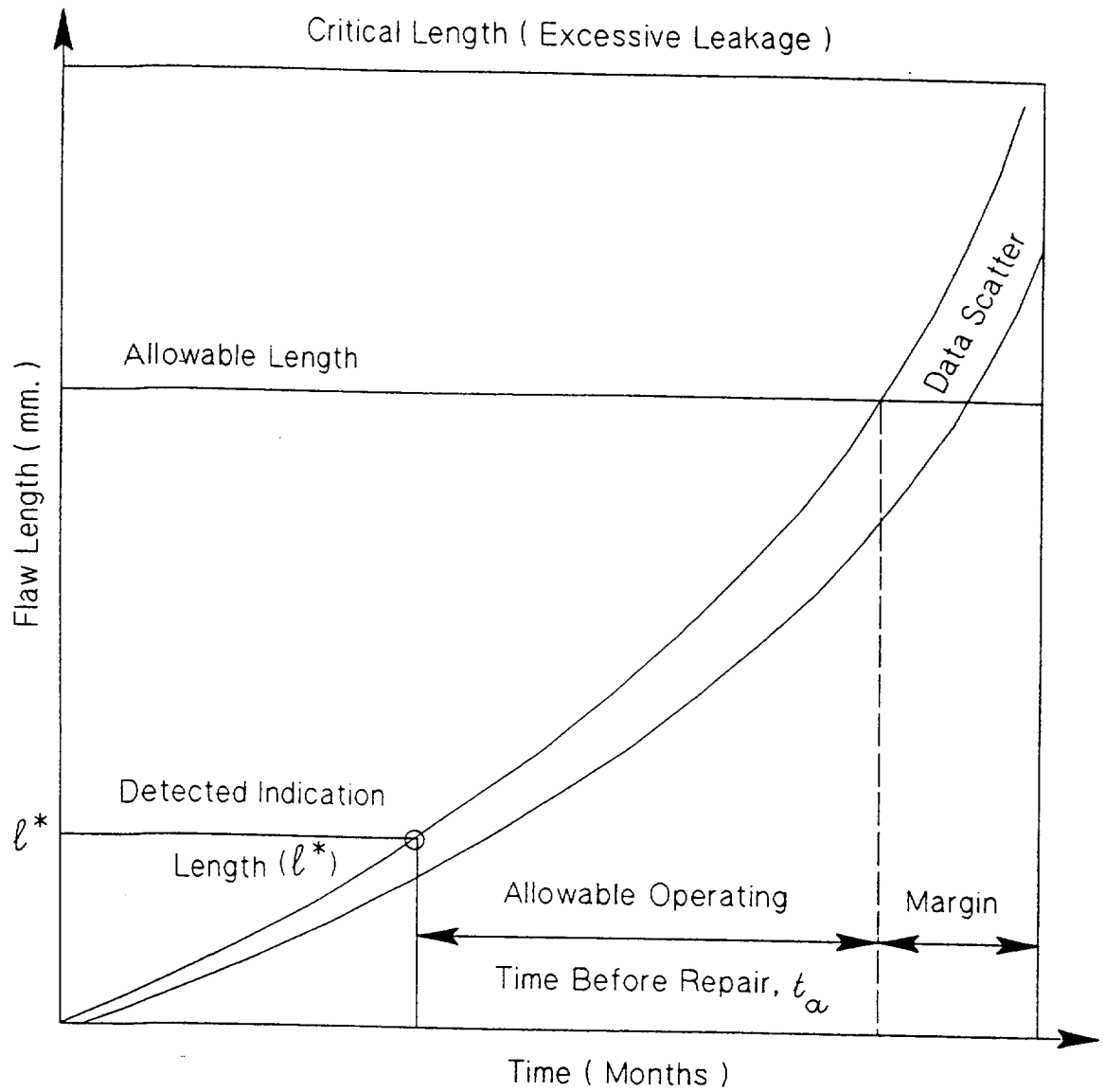

FIGURE 3-2

SCHEMATIC OF A HEAD PENETRATION FLAW TOLERANCE CHART

FOR THROUGH-WALL FLAWS

SECTION 4.0

MATERIAL PROPERTIES, FABRICATION HISTORY AND CRACK GROWTH PREDICTION

4.1 MATERIALS AND FABRICATION

The chemical analysis, mechanical properties and heat treatment of the Alloy 600 material used to fabricate the four vessels head penetrations are provided in Tables 4-1 through 4-4. The material CMTRs were used to obtain the chemistry and mechanical properties for the vessel head penetrations. The CMTRs for the material indicate the heat treatment of the material in most cases, except for the B&W heats, which are presently being researched.

The head adapters for North Anna and Surry Units were manufactured by Rotterdam Dockyard. The North Anna Units were fabricated from material produced by Sanvik in Sweden. The penetrations for Surry Unit 1 originated at Huntington Alloys, while those for Surry Unit 2 came from Babcock and Wilcox Tubular Products and Sanvik, as shown in Tables 4-3 and 4-4. Figures 4-1 and 4-2 illustrate the yield strengths and carbon content, based on percent of heats, of the head adapter penetrations in the North Anna and Surry Units vessel relative to a sample of the French head penetrations which have experienced cracking. The head penetrations in the North Anna and Surry Units have a higher carbon content, higher mill annealing temperature and lower yield strength relative to the French penetrations. These factors should all have a beneficial effect on the material resistance to PWSCC in the head penetrations.

4.2 CRACK GROWTH PREDICTION

The cracks in the penetration region have been determined to result from primary water stress corrosion cracking in the Alloy 600 base metal. There are a number of available measurements of static load crack growth rates in primary water environment, and in this section the available results will be compared and a representative growth rate established.

Direct measurements of SCC growth rates in Alloy 600 are relatively rare, and care should be used in interpreting the results because the materials may be excessively cold worked, or the loadings applied may be near or exceeding the limit load of the tube, meaning there will be an interaction between tearing and crack growth. In these cases the crack growth rates may not be representative of service conditions.

The effort to develop a reliable crack growth rate model for Alloy 600 began in the Spring of 1992, when the Westinghouse Owners Group was developing a safety case to support continued operation of plants. At the time there was no available crack growth rate data for head penetration materials, and only a few publications existed on growth rates of Alloy 600 in any product form.

The best available publication was found to be that of Peter Scott of Framatome, who had developed a growth rate model for PWR steam generator materials [1]. His model was based on a study of results obtained by McIlree and Smialowska [2] who had tested short steam generator tubes which had been flattened into thin compact specimens. His results are shown in Figure 4-3. Upon study of his paper there were several ambiguities, and several phone conversations were held to clarify his conclusions. These discussions led to Scott's admission that reference 1 contains an error, in that no correction for cold work was applied to the McIllree/Smialowska data. The correct development is below.

An equation was fitted to the data of reference [2] for the results obtained in water chemistries that fell in within the standard specification. Results for chemistries outside the specification were not used. The following equation was fitted to the data:

$$\frac{da}{dt} = 2.8 \times 10^{-11} (K-9)^{1.16} \text{ m/sec}$$

where K is in MPa$\sqrt{m}$.

The next step described by Scott in his paper was to correct these results for the effects of cold work. Based on work by Cassagne and Gelpi [3], he concluded that dividing the above equation by a factor of 10 would be appropriate to account for the effects of cold work. This step was inadvertently omitted from Scott's paper, even though it is discussed. The crack growth law for 330°C then becomes:

$$\frac{da}{dt} = 2.8 \times 10^{-12} (K-9)^{1.16} \text{ m/sec}$$

This equation was verified by Scott in a phone call in July 1992.

Scott further corrected this law for the effects of temperature, but his correction was not used in the model employed here. Instead, an independent temperature correction was developed based on service experience. This correction uses an activation energy of 33 kCal/mole, which gives a smaller temperature correction than that used by Scott (44 kcal/mole), and will be discussed in more detail below.

Scott's crack growth law is shown for 330°C in Figure 4-3, and this law was independently obtained by B. Woodman of ABB-CE, who went back to the original data base, and did not account for cold work. His equation was of a slightly different form:

$$\frac{da}{dt} = 0.2 \exp [A + B \ln \{\ln (K-Q)\}]$$

Where $A = -25.942$

$B = 3.595$

$Q = 0$

This equation is nearly identical with Peter Scott's original model uncorrected for cold work. This work provided an independent verification of Scott's work.

The final proof of the usefulness of Peter Scott's model comes from actual data from head penetration materials. A testing program was carried out at Westinghouse in the mid-1990s, and 18 heats were tested in carefully controlled PWR environment. The results of the program are published in reference [4]. One heat did not crack, and of the seventeen heats where cracking was observed, the growth rates observed in fourteen were bounded by the modified Scott model. Three heats cracked at a faster rate, and the explanation for this behavior is being investigated. These three heats are different both in source and product form from those in the Surry and North Anna plants.

Since the North Anna and Surry Units operate at 600°F (316°C) or slightly lower in the head region [9,10,13], and the crack growth rate is strongly affected by temperature, a temperature adjustment is necessary. This temperature correction was obtained from study of both laboratory and field data for stress corrosion crack growth rates for Alloy 600 in primary water environments. The available data are summarized in Figure 4-4, where most of the results are from steam generator tube materials, with several

sets of data from operating plants. Some of the points (the solid circles) were obtained from cracking which was found in head penetrations in operating plants.

The data shown in Figure 4-4 results in an activation energy of 33 Kcal/mole, which can be used to adjust for the lower operating temperature. This value is slightly lower than the generally accepted activation energy of 44-50 Kcal/mole used to characterize the effect of temperature on crack initiation, but the trend of the actual data for many different sources is unmistakable.

Use of the 33 Kcal/mole activation energy results in a correction factor 0.526 for crack growth rates at 316°C, compared to the rate at 330°C. Therefore the following growth rate model was used for the Surry and North Anna head penetrations:

$$\frac{da}{dt} = 1.473\times10^{-12}(K-9)^{1.16} \text{ m/sec}$$

where K = applied stress intensity factor, in $MPa\sqrt{m}$. This equation implies a threshold for cracking susceptibility, $K_{ISCC} = 9\ MPa\sqrt{m}$.

a,c,e

a,c,e

a,c,e

a,c,e

a,c,e

a,c,e

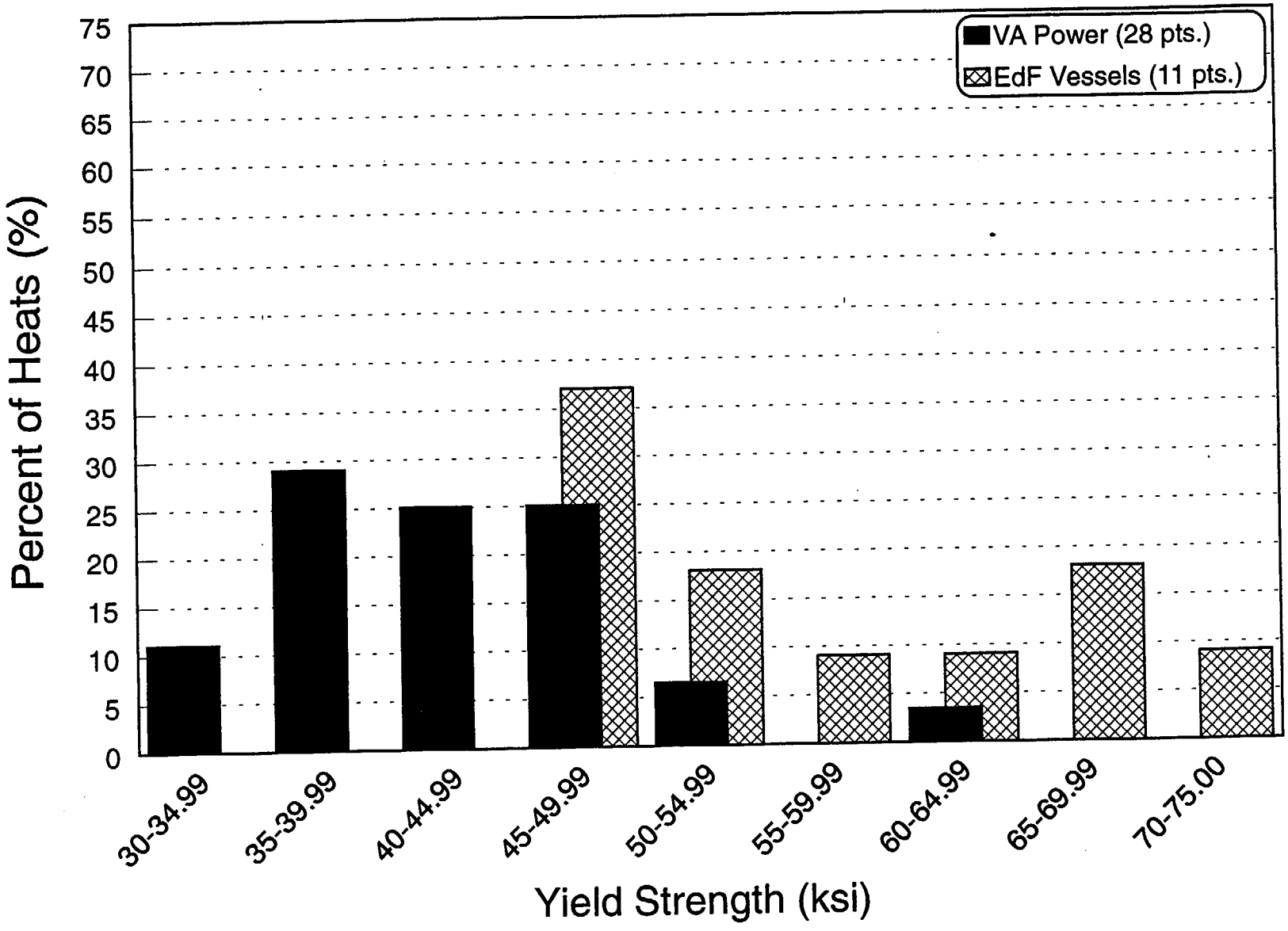

FIGURE 4-1

YIELD STRENGTH OF THE VARIOUS HEATS OF ALLOY 600 USED IN

FABRICATING THE NORTH ANNA AND SURRY UNITS AND FRENCH HEAD ADAPTOR PENETRATIONS

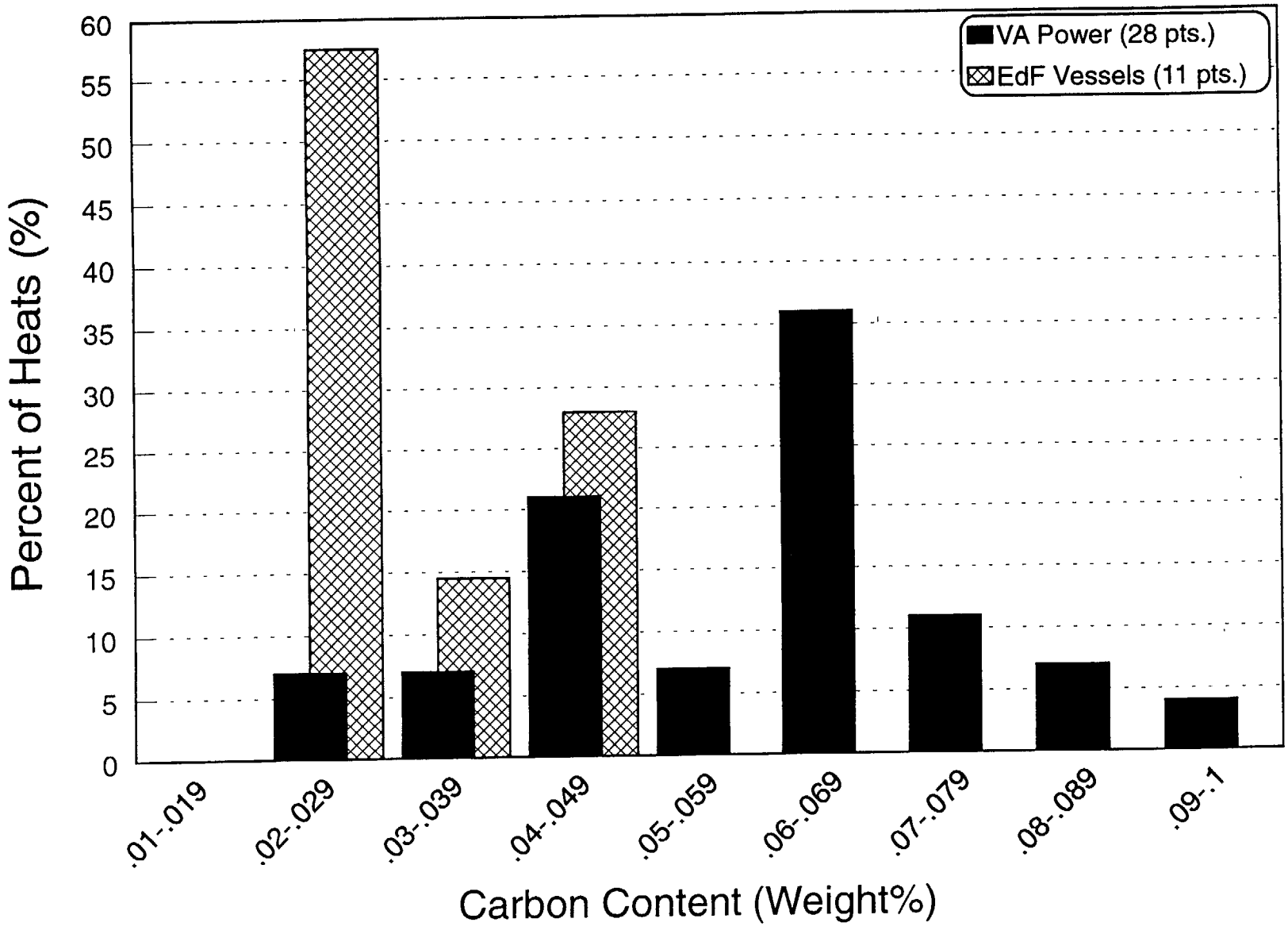

FIGURE 4-2

CARBON CONTENT OF THE VARIOUS HEATS OF ALLOY 600 USED IN FABRICATING THE NORTH ANNA AND SURRY UNITS AND FRENCH HEAD ADAPTOR PENETRATIONS

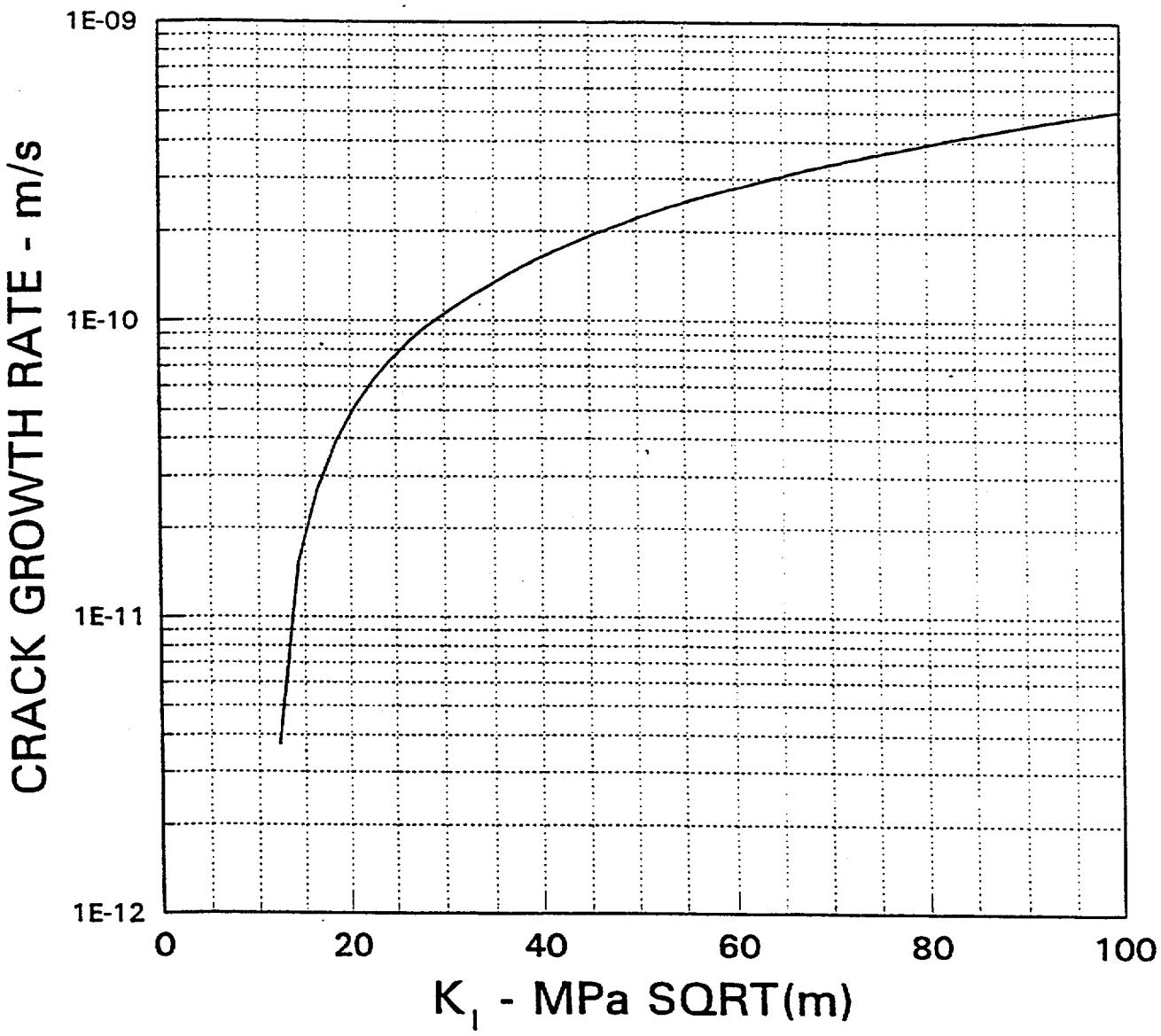

FIGURE 4-3

SCOTT'S MODEL[1] FOR SCC GROWTH RATES IN ALLOY 600 IN PRIMARY WATER ENVIRONMENTS (330°C)

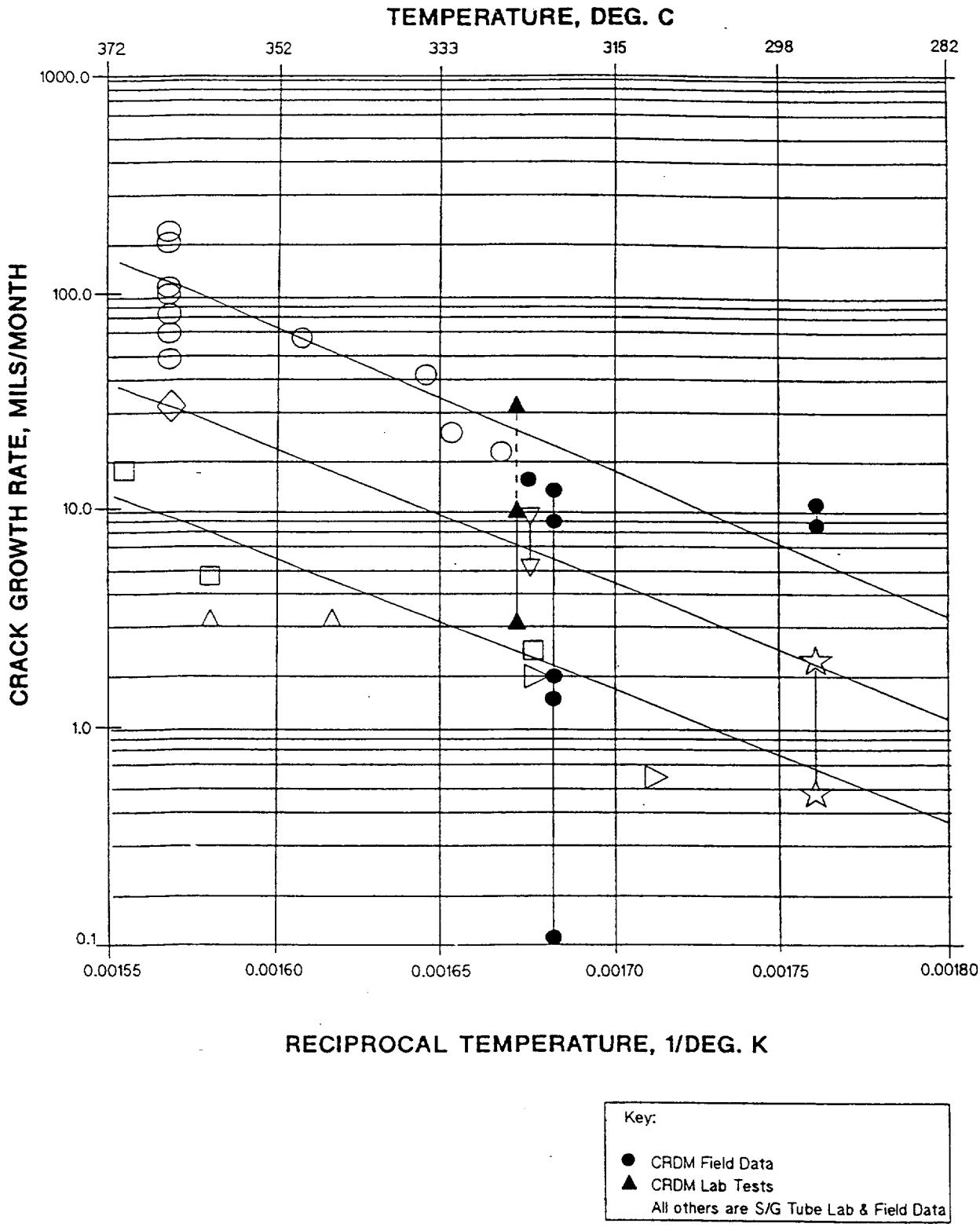

FIGURE 4-4

SUMMARY OF TEMPERATURE EFFECTS ON SCC GROWTH RATES FOR ALLOY 600 IN PRIMARY WATER, LABORATORY AND FIELD EXPERIENCE

SECTION 5.0
STRESS ANALYSIS

5.1 OBJECTIVES OF THE ANALYSIS

The objective of this analysis was to obtain accurate stresses at and near each CRDM housing. To do so requires a three dimensional analysis which considers all the loadings on the penetration[6]. An investigation of deformations at the lower end of the housing was also performed using the same model. Three locations were considered: the outermost row, the next outermost row, and the center location.

The analyses provided information for the flaw tolerance evaluation in Section 6. Also, the results of the stress analysis were compared to the findings from service experience, to help assess the causes of the cracking which has been observed.

5.2 MODEL

Three dimensional finite element models comprised of isoparametric brick and wedge elements with midside nodes on each face were used to obtain the stresses and deflections. A view of the unstressed model for the outermost row is shown in Figure 5-1. Taking advantage of symmetry through the vessel and penetration centerlines, only half of the penetration geometry plus the surrounding vessel were modeled for the outermost and next outermost penetrations. For the center penetration, it was necessary to model only one-quarter of the penetration as opposed to one-half of the penetration. The difference between the hillside penetrations and the center penetration was that there was no differential height across the weld for the center penetration.

The lower portion of the Control Rod Drive Mechanism (CRDM) Adapter tube (i.e., penetration tube), the adjacent section of the vessel closure head, and the joining weld were modeled. The vessel to penetration tube weld was simulated with two layers of elements. The penetration tube, weld metal and cladding were modeled as Alloy 600 and the vessel head shell as carbon steel.

5.3 STRESS ANALYSIS RESULTS - OUTERMOST PENETRATION

Figure 5-2 shows the outward displacement of the entire model for the steady state condition. For the steady state, the tube OD is pressing on the vessel (i.e. couple each tube node, except for the vertical

direction, to its neighbor in the vessel). Figure 5-3 presents the hoop stresses for the steady state condition.

[

]a,c,e

5.4 STRESS ANALYSIS RESULTS - NEXT OUTERMOST PENETRATION

[

]a,c,e

5.5 STRESS ANALYSIS RESULTS - CENTER PENETRATION

[

]a,c,e

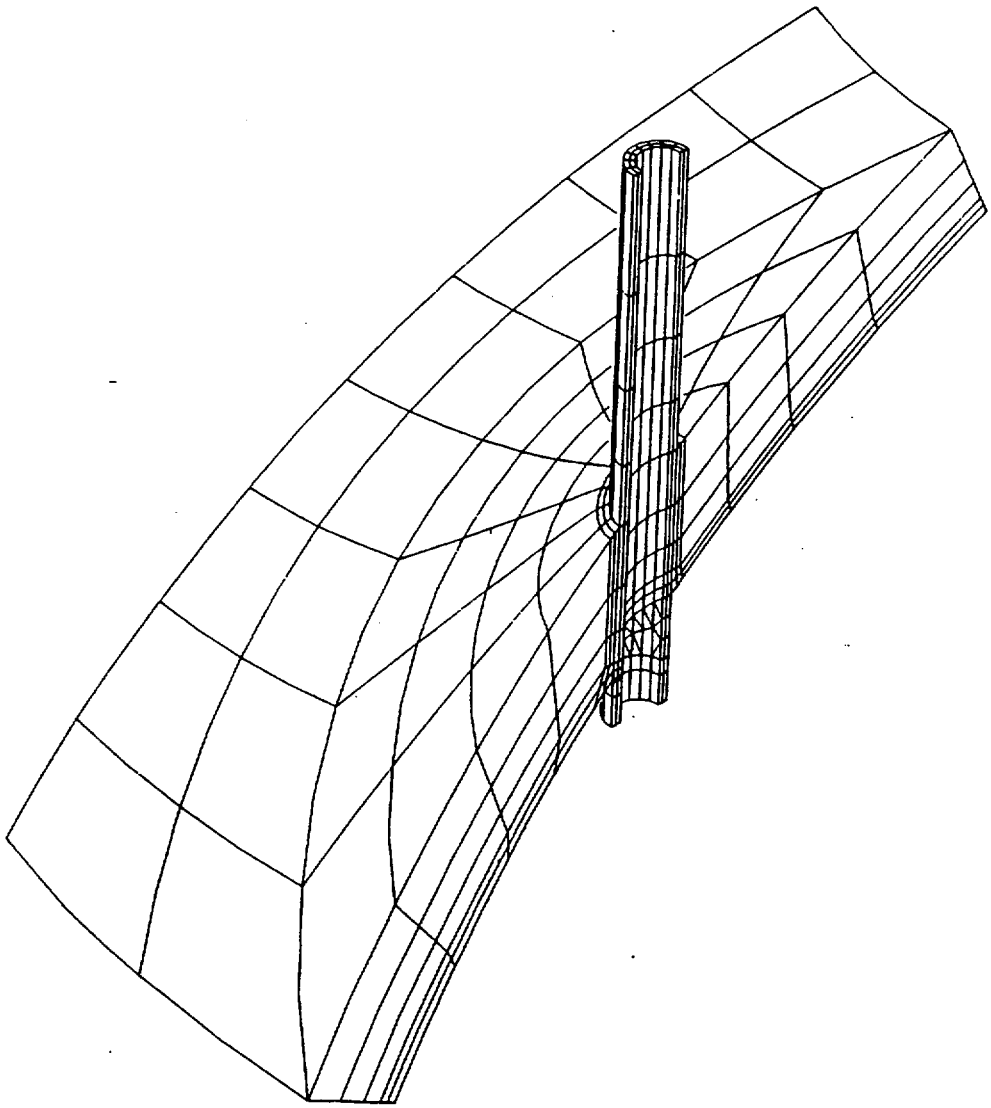

FIGURE 5-1

THREE-DIMENSIONAL MODEL OF THE OUTERMOST PENETRATION

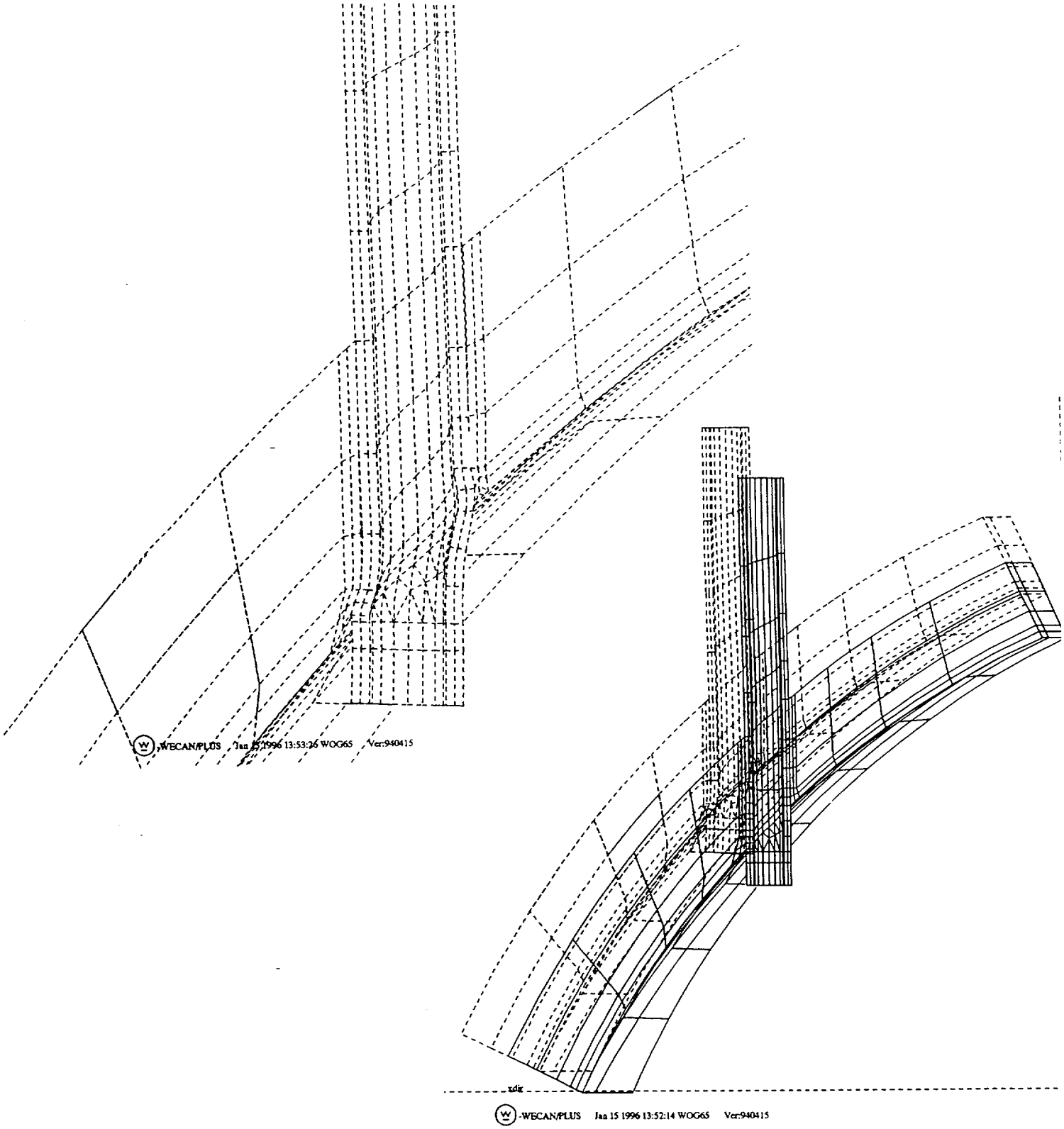

FIGURE 5-2

STEADY STATE DISPLACEMENT OF R/V CLOSURE HEAD AND OUTERMOST PENETRATION

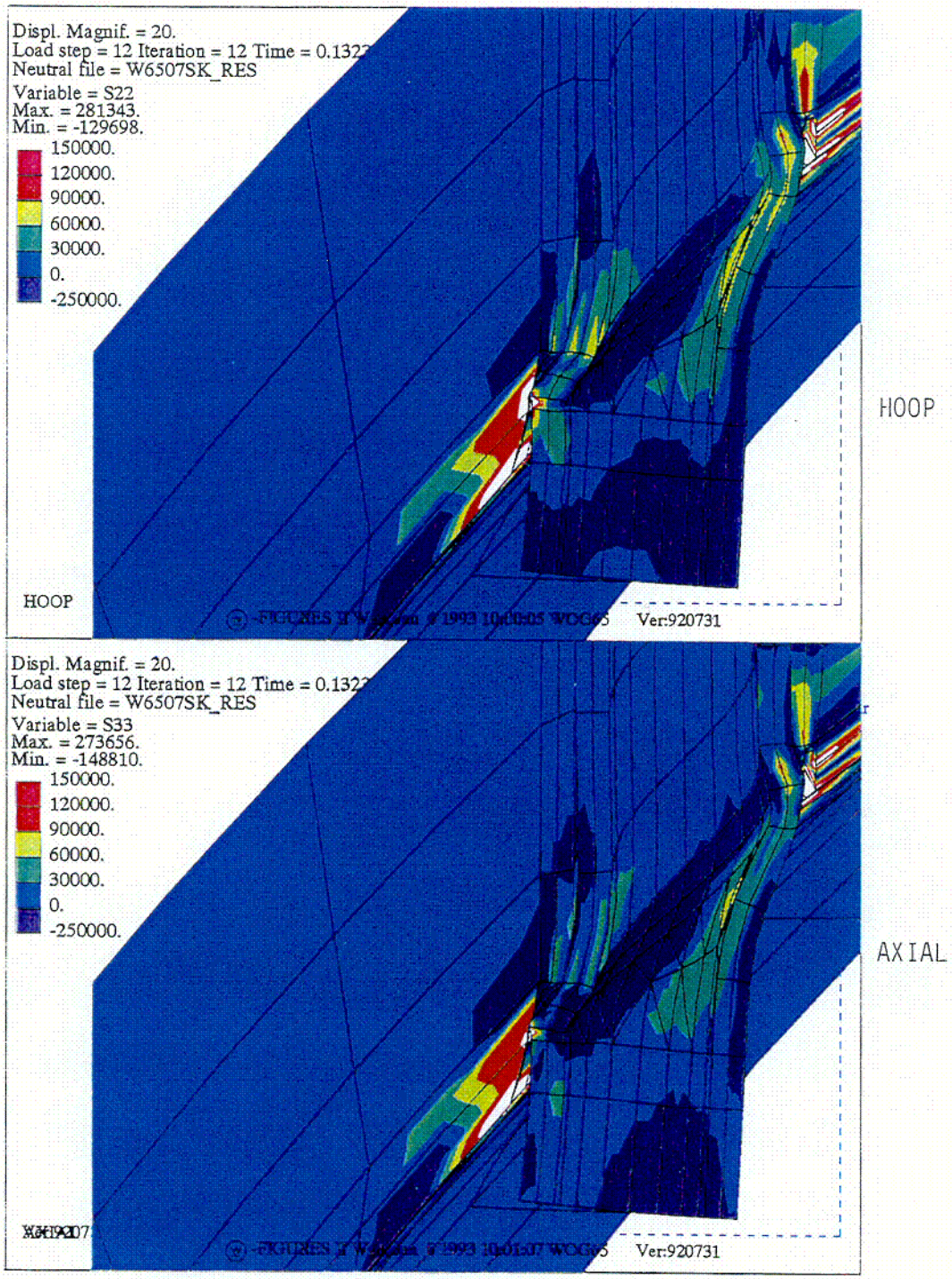

FIGURE 5-3

STRESS DISTRIBUTION AT STEADY STATE CONDITIONS: OUTERMOST PENETRATION

C01

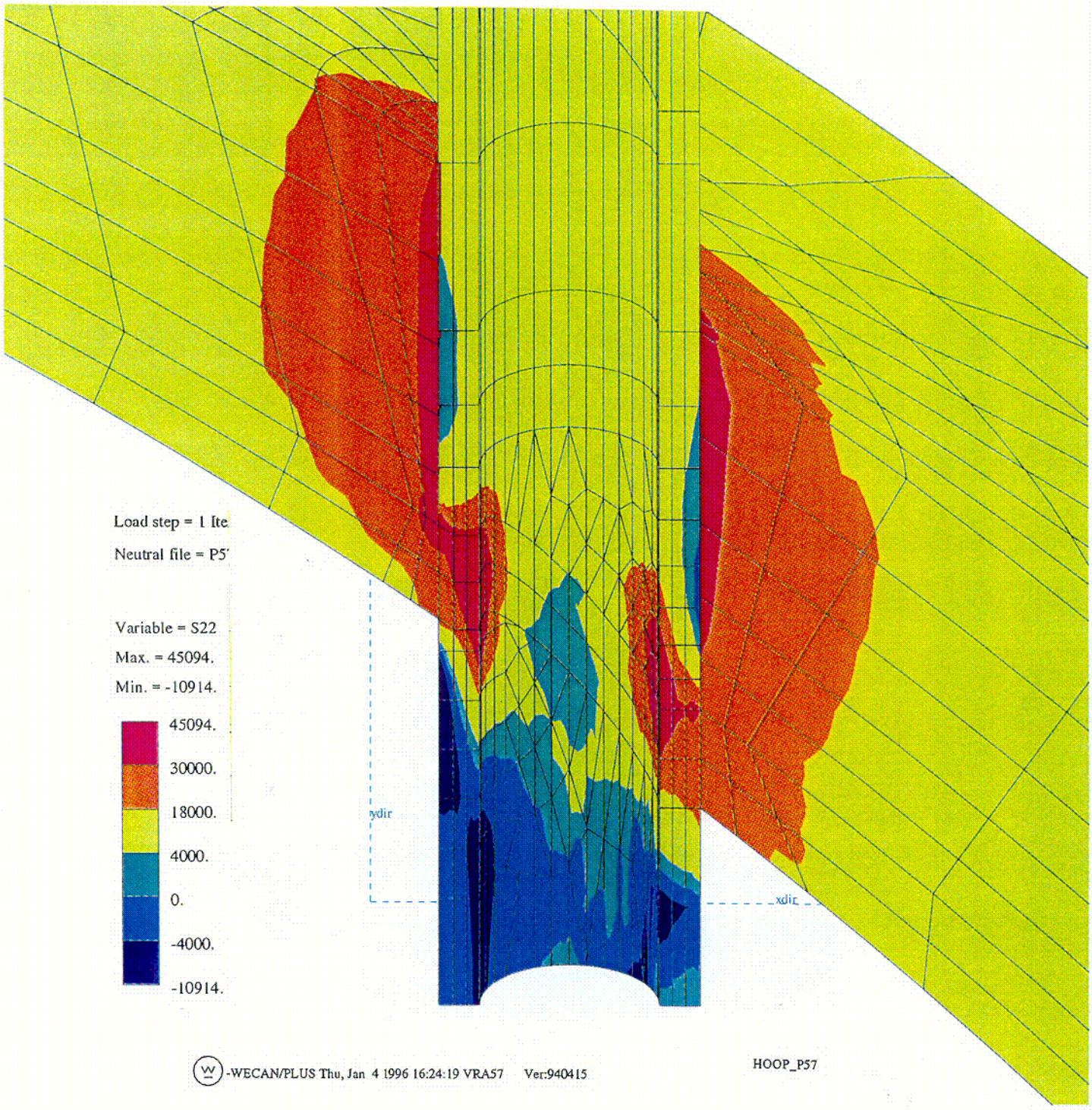

FIGURE 5-4

HOOP STRESS CONTOUR PLOTS ALONG THE NEXT OUTERMOST PENETRATION

C02

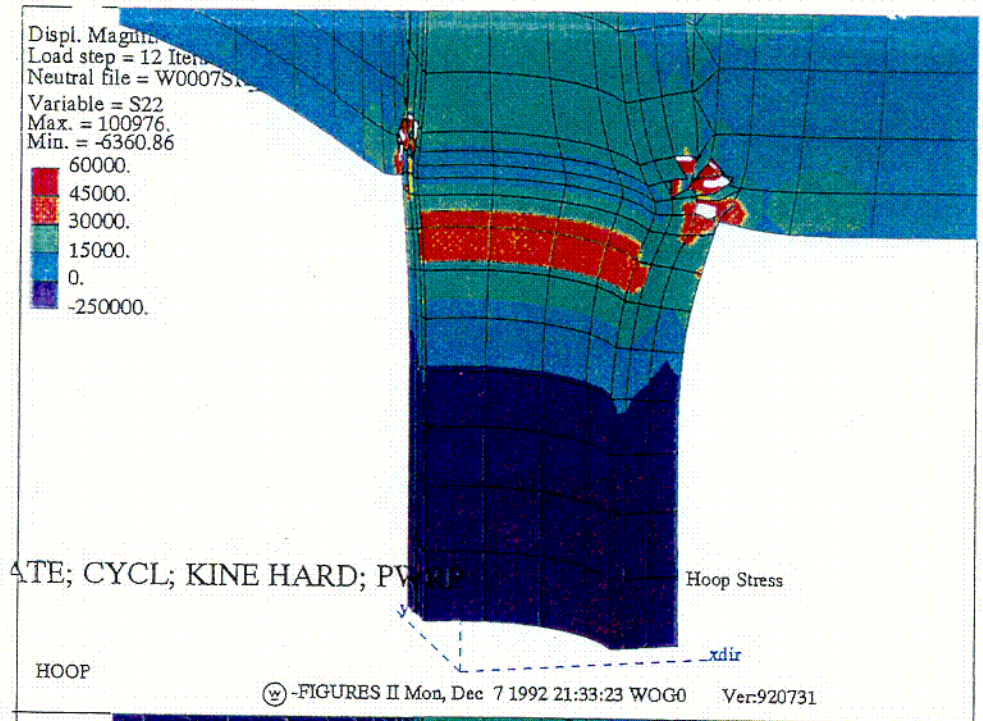

HOOP

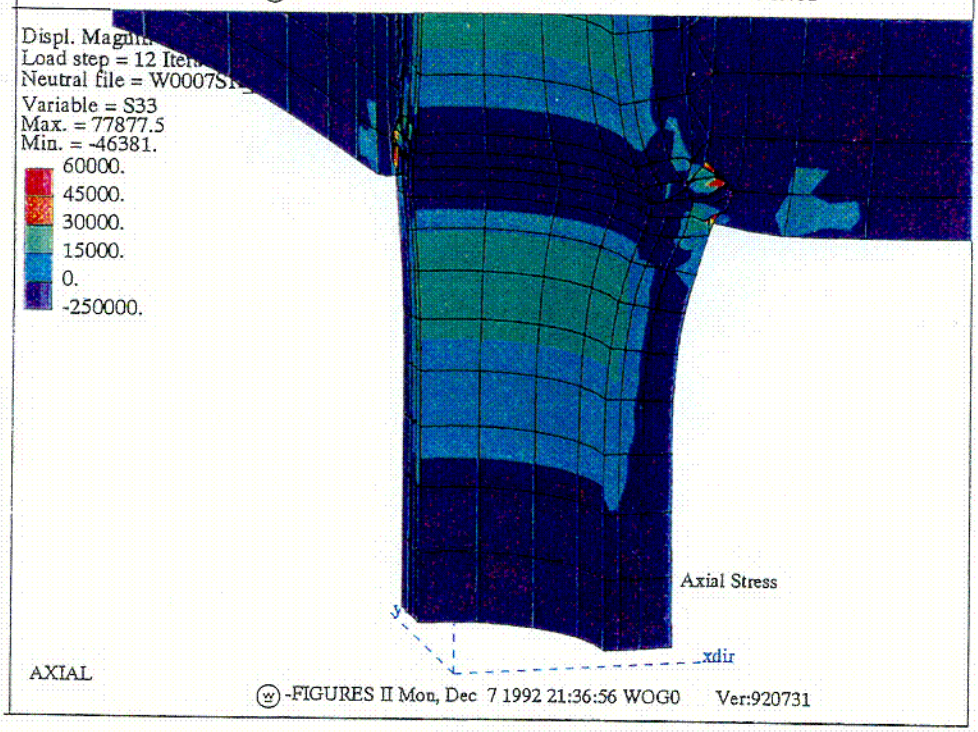

AXIAL

FIGURE 5-5

STRESS DISTRIBUTION AT STEADY STATE CONDITION FOR THE CENTER PENETRATION

C03

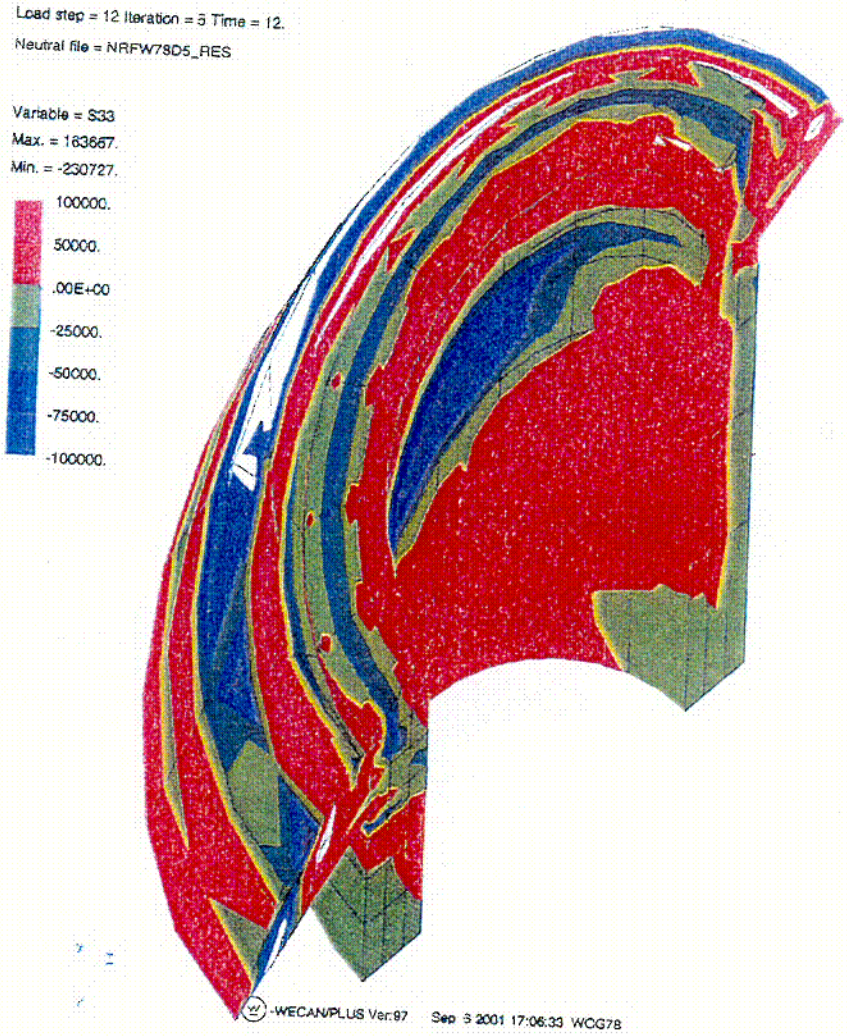

FIGURE 5-6

STRESS DISTRIBUTION AT STEADY STATE FOR THE OUTERMOST PENETRATION, ALONG A PLANE ORIENTED PARALLEL TO, AND JUST ABOVE, THE ATTACHMENT WELD

SECTION 6.0
FLAW EVALUATION CHARTS

6.1 INTRODUCTION

The flaw evaluation charts were developed from the stress analysis of each of the penetration locations, as discussed in Section 5. The crack growth law developed in Section 4.2 was used for each case, and two flaw tolerance charts were developed for each penetration location. The first chart characterizes the growth of a part-through flaw in the thickness direction, and the second chart characterizes the growth of a through-wall flaw in the length direction. The allowable remaining life of the penetration may then be directly determined, using the combined results of the two charts. All times resulting from these calculations are effective full power years.

Inspection tolerance. It is important to describe the treatment of inspection tolerances in this report. The flaw evaluation charts are designed to be best estimate predictions of the future propagation of flaws. The initial flaw size used in these charts should be a best estimate of the actual flaw size. Appropriate safety margins are incorporated into the acceptance criteria described in Section 6.5, so no additional margins on the flaw size or position are required. This approach is consistent with that used throughout the flaw evaluation process in Section XI of the ASME Code.

6.2 OVERALL APPROACH

The results of the three-dimensional stress analysis of the penetration locations were used directly in the flaw tolerance evaluation. The maximum stress is the hoop stress, and the flaws which have been found inservice are all longitudinally oriented, so the hoop stress component was used.

The crack growth evaluation for the part-through flaws was based on the stress distribution through the penetration wall at the location which corresponds to the highest stress along the inner surface of the penetration. The highest stressed location was found to be in the immediate vicinity of the weld for all penetrations.

The stress profile was represented by a cubic polynomial:

$$\sigma(x) = A_0 + A_1 \frac{x}{t} + A_2 \left(\frac{x}{t}\right)^2 + A_3 \left(\frac{x}{t}\right)^3$$

where	x	=	is the coordinate distance into the wall
	t	=	wall thickness
	σ	=	stress perpendicular to the plane of the crack
	A_i	=	coefficients of the cubic fit

For the surface flaw with a length six times its depth, the stress intensity factor expression of McGowan and Raymund [5A] was used. The stress intensity factor $K_I(\varphi)$ can be calculated anywhere along the crack front. The point of maximum crack depth is represented by $\varphi = 0$. The following expression is used for calculating $K_I(\varphi)$, where φ is the angular location around the crack.

$$K_I(\varphi) = \left[\frac{\pi a}{Q}\right]^{0.5} (\cos^2\varphi + \frac{a^2}{C^2} \sin^2\varphi)^{1/4} (A_O H_O + \frac{2}{\pi}\frac{a}{t} A_1 H_1$$

$$+ \frac{1}{2}\frac{a^2}{t^2} A_2 H_2 + \frac{4}{3\pi}\frac{a^3}{t^3} A_3 H_3)$$

The magnification factors $H_O(\varphi)$, $H_1(\varphi)$, $H_2(\varphi)$ and $H_3(\varphi)$ are obtained by the procedure outlined in reference [5A]. The parameter C is the flaw half-length.

[

$$K = \sigma (\pi a)^{0.5}$$

]a,c,e

[

]a,c,e

The results discussed in the following sections have been designed to provide crack growth predictions for a range of flaw sizes, locations and orientations. A simple flow chart for determination of which figure to use is shown in Table 6-2.

6.3 RESULTS: AXIAL FLAWS

Surface Flaws

The results of the calculated growth through the wall for inside surface axial flaws postulated in the penetrations are summarized in Figures 6-1a and 6-1b. Figures 6-1a, 6-1b, and 6-1c apply to surface crack locations anywhere in the weld region of any of the penetrations, since the stress results were taken at the highest stressed location, which is in the outermost penetration. Figure 6-1a is a prediction of crack growth at and below the attachment weld region, while the Figure 6-1b covers crack growth above the weld. Figure 6-1c applies to crack growth for outside surface axial flaws, regardless of location. Note that the predicted extension through the penetration thickness requires many years at the operating temperature for North Anna and Surry Units, regardless of the location.

Through-Wall Flaws

Figure 6-2 and 6-3 present the predicted crack growth for a through-wall flaw postulated to exist below the weld region in the outermost penetration. These results are for the lower hillside and centerside locations respectively. Although there are different levels of ovality (and therefore residual stress) in the different penetrations, it is clear that in the vicinity of the weld and below it, the total stresses approach the yield stress of the material, which was set at 378.6 MPa (55 ksi) for this calculation. Figures 6-4 and 6-5 provide similar results for the next outermost row of penetrations.

Figure 6-6 provides projections of growth above the weld region for the center penetration. The upper edge of the weld has been assumed to be at the 2.0 inch location in this figure, and the growth above this location is presented as a function of time in years.

Note that for some of the penetrations, crack extension actually stops. This occurs as the stress intensity factor decreases with the lower stresses, to a value below the threshold cracking susceptibility value of 9 MPa $\sqrt{m}$.

6.4 CIRCUMFERENTIAL CRACK PROPAGATION

Since circumferentially oriented flaws have been found at three plants (Bugey 3, Oconee 2, and Oconee 3), it is important to consider the possibility of crack extension in the circumferential direction. The first case was discovered as part of the destructive examination of the tube with the most extensive longitudinal cracking at Bugey 3, and the crack was found to have extended to a depth of 2.25 mm in a wall thickness of 16 mm. The flaw was found at the outside surface of the penetration (number 54) at the lower hillside location, just above the weld.

The circumferential flaws in Oconee Unit 3 were discovered during the process of repairing a number of axial flaws, while the circumferential flaw in Oconee Unit 2 was discovered by UT. Experience gained from these findings has enabled the development of UT procedures capable of detecting circumferential flaws reliably.

It is important to realize that a flaw would have to propagate through the penetration or the attachment weld, and result in a leak, before the outer surface of the penetration would be exposed to the water. Cracking could then begin for an outside surface flaw. (This is believed to have been the case at all three plants in which circumferential flaws were found). This time period was conservatively ignored in the calculations to be discussed.

To investigate this issue completely, a series of crack growth calculations were carried out for a postulated surface circumferential flaw located just above the head penetration weld, in a plane parallel to the weld itself. This is the only flaw plane which could result in a complete separation of the penetration. All others would result in propagation below the weld, and therefore no chance of complete separation because the remaining weld would hold the penetration in place.

[

]a,c,e

[

]a,c,e

The time required for propagation of a circumferential flaw to a point where the integrity of the penetration would be affected would therefore be at least 26 years, as shown in Figure 6-8. Because of the conservatisms in the calculations, as discussed above, it is likely to be even longer.

6.5 FLAW ACCEPTANCE CRITERIA

Now that projected crack growth curves have been developed, the question which remains to be addressed is what size flaw would be acceptable for further service.

Acceptance criteria have been developed for indications found during inspection of reactor vessel upper head penetrations. These criteria were developed as part of an industry program coordinated by NUMARC (now NEI). Such criteria are normally found in Section XI of the ASME Code, but Section XI does not require inservice inspection of these regions and therefore acceptance criteria are not

available. In developing the enclosed acceptance criteria, the approach used was very similar to that used by Section XI, in that an industry consensus was reached using input from both operating utility technical staff and each of the three PWR vendors. The criteria developed are applicable to all PWR plant designs.

Since the discovery of the leaks at Oconee and ANO-1, the acceptance criteria have been revised slightly, to cover flaws on the outside diameter of the penetration below the attachment weld, and flaws in the attachment weld. These revised criteria are now in draft form, but they are expected to be acceptable to the NRC, and will be used in these evaluations. The draft portions of the acceptance criteria will be noted below.

The criteria which are presented herein are limits on flaw sizes which are acceptable. The criteria are to be applied to inspection results. It should be noted that determination of the future service time during which the criteria are satisfied is plant-specific and dependent on flaw geometry and loading conditions.

It has been previously demonstrated by each of the owners groups that the penetrations are very tolerant of flaws and there is only a small likelihood of flaw extension to large sizes. Therefore, it was concluded that complete fracture of the penetration is highly unlikely and, therefore, protection against leakage during service is the priority.

The approach used here is more conservative than that used in Section XI applications, where the acceptable flaw size is calculated using a margin on the critical flaw size. In this case, the critical flaw size is far too large to allow a practical application of this approach, so protection against leakage is the key element.

The acceptance criteria apply to all flaw types regardless of orientation or shape. The same approach is used by Section XI, where flaws are characterized according to established rules and then compared with acceptance criteria.

Flaw Characterization

Flaws detected must be characterized by length and preferably depth. If only the length is determined, assume the depth is half the length based on experience with the shape of flaws reported. The proximity rules of Section XI for considering flaws as separate, may be used directly (Section XI, Figure IWA 3400-1). This figure is reproduced here as Figure 6-9.

When a flaw is found, its projections in both the axial and circumferential directions must be determined. Note that the axial direction is always the same for each penetration, but the circumferential direction will be different depending on the angle of intersection of the penetration with the head. The "circumferential" direction of interest here is along the top of the attachment weld, as illustrated in Figure 6-10. It is this angle which will change for each penetration and which is also the plane which could cause separation of the penetration tube from the head. The location of the flaw relative to both the top and bottom of the partial penetration attachment weld must be determined since a potential leak path exists when a flaw progresses through the wall and up the penetration past this weld. A schematic of a typical weld geometry is shown in Figure 6-11.

Flaw Acceptance Criteria

The maximum allowable depth (a_f) for flaws on the inside surface of the penetration, at or above the weld is 75 percent of the penetration wall thickness regardless of the flaw orientation. The term a_f is defined as the maximum size to which the detected flaw is calculated to grow in a specified time period. This 75 percent limitation was selected to be consistent with the maximum acceptable flaw depth in Section X1 and to provide an additional margin against through wall penetration. There is no concern about separation of the head penetration from the head, unless the flaw is above the attachment weld and oriented circumferentially. Calculations have been completed to show that all penetration geometries can support a continuous circumferential flaw with a depth of 75 percent of the wall.

Axial inside surface flaws found below the weld are acceptable regardless of depth as long as their upper extremity does not reach the bottom of the weld during the period of service until the next inspection. Axial flaws which extend above the weld are limited to 75 percent of the wall.

Axial flaws on the OD of the penetration below the attachment weld are acceptable regardless of depth, as long as they do not extend into the attachment weld during the period of service until next inspection. Axial OD flaws above the attachment weld must be evaluated on a case by case basis, and must be discussed with the regulatory authority.

Circumferential flaws located below the weld are acceptable regardless of their depth, provided the length is less than 75 percent of the circumference for the period of service until the next inspection. Flaws in this area have no structural significance but loose parts must be avoided. To this end,

intersecting axial and circumferential flaws shall be removed or repaired. Circumferential flaws at and above the weld must be discussed with the regulatory authority on a case by case basis.

Flaws located in the attachment welds themselves are not acceptable regardless of their depth. This is because the crack propagation rate is several times faster than that of the Alloy 600 tube material, and also because depth sizing capability does not yet exist for indications in the weld.

These criteria are summarized in Table 6-1. Flaws which exceed these criteria must be repaired unless analytically justified for further service. These criteria have been reviewed and approved by the NRC, as documented in references 7 and 8, with the exception of the draft criteria discussed above, for OD flaws and flaws in the attachment weld.

It is expected that the use of these criteria and crack growth curves will provide conservative predictions of the allowable time of service. Similar criteria have been proposed in Sweden and France, and are under discussion in other countries.

TABLE 6-1 SUMMARY OF R.V. HEAD PENETRATION ACCEPTANCE CRITERIA				
Location	Axial		Circ	
	a_f	ℓ	a_f	ℓ
Below Weld (ID)	t	no limit	t	.75 circ.
At and Above Weld (ID)	0.75 t	no limit	*	*
Below Weld (OD)	t	no limit	t	.75 circ.
Above Weld (OD)	*	*	*	*

a_f = Flaw Depth as defined in IWB 3600

ℓ = Flaw Length

t = Wall Thickness

Note: Flaws of any size are not acceptable in the attachment weld itself.

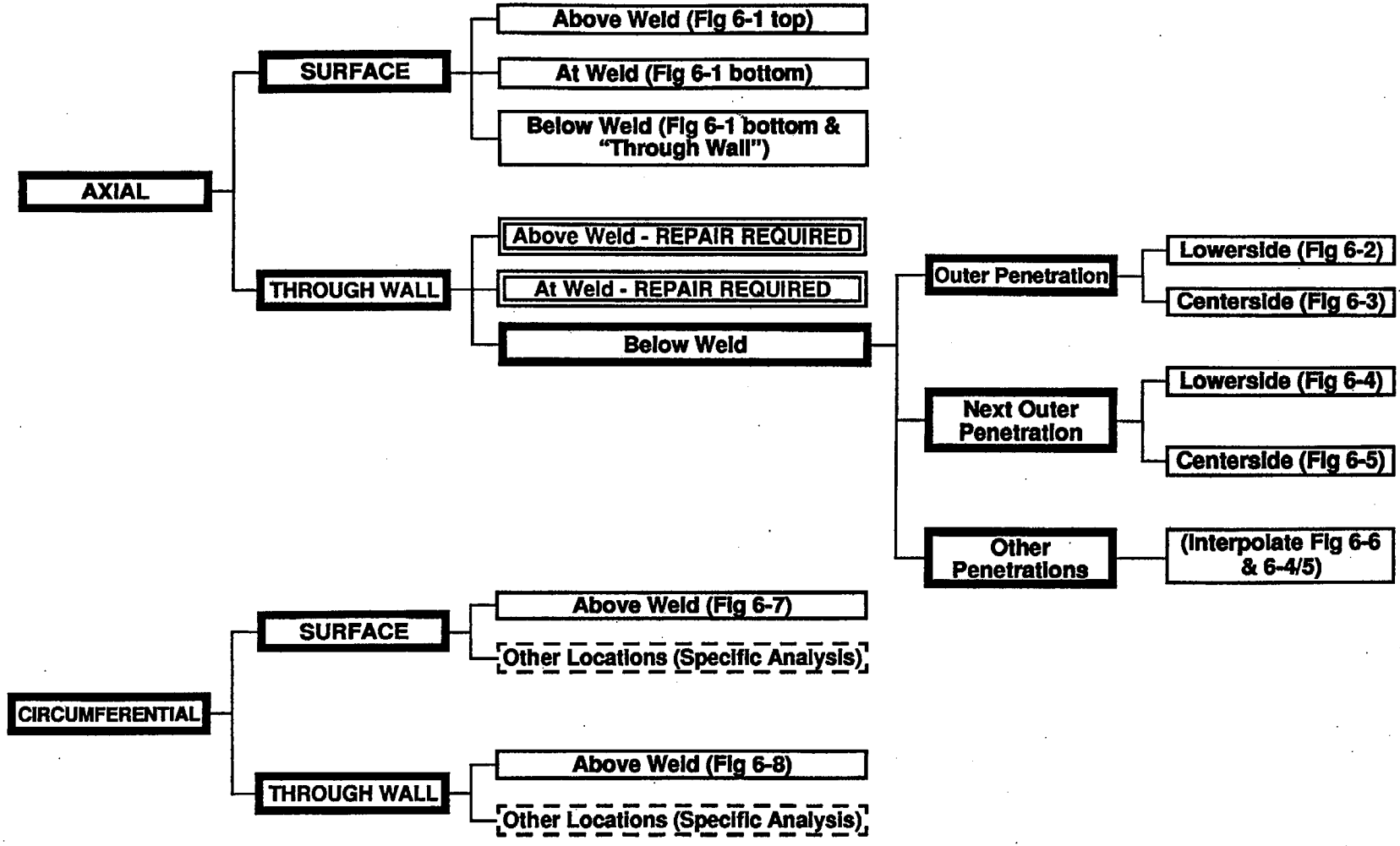

TABLE 6-2
GUIDELINES FOR CHOICE OF FLAW EVALUATION CHARTS

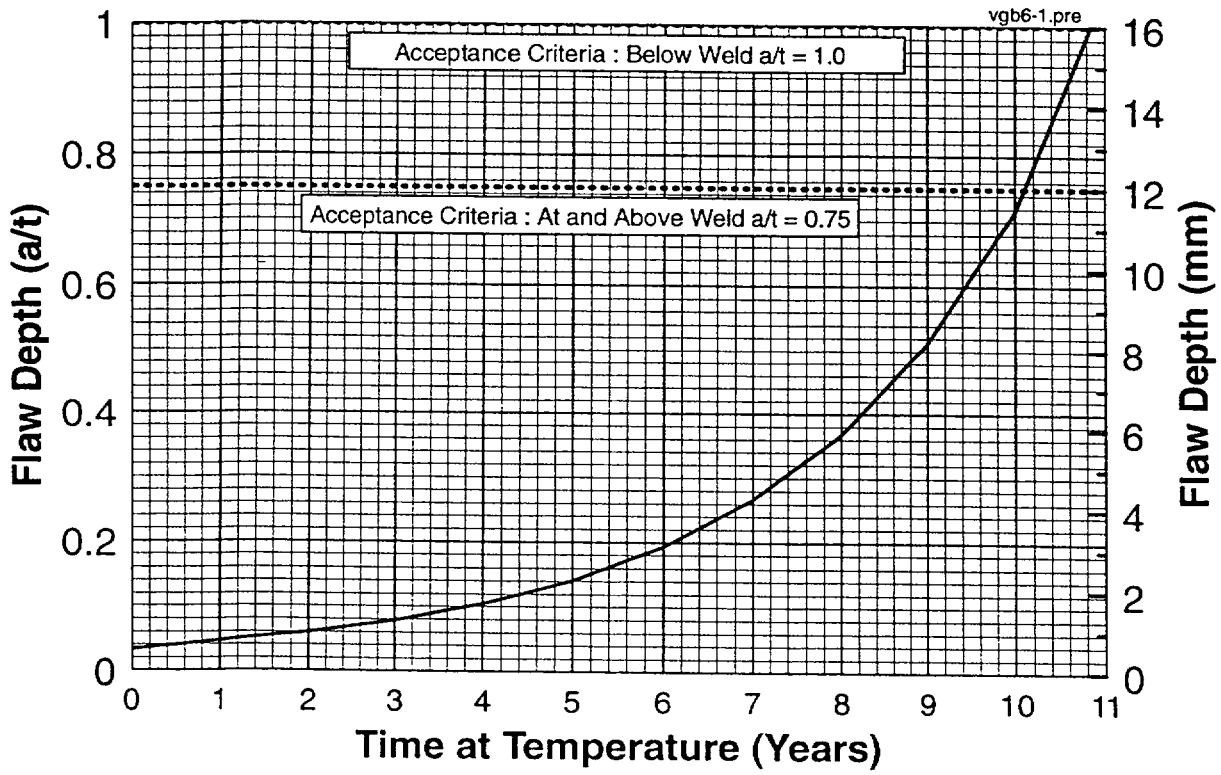

FIGURE 6-1a

CRACK GROWTH PREDICTIONS FOR LONGITUDINAL INSIDE SURFACE FLAWS IN THE HEAD PENETRATIONS AT THE NORTH ANNA AND SURRY UNITS, AT AND BELOW THE ATTACHMENT WELD

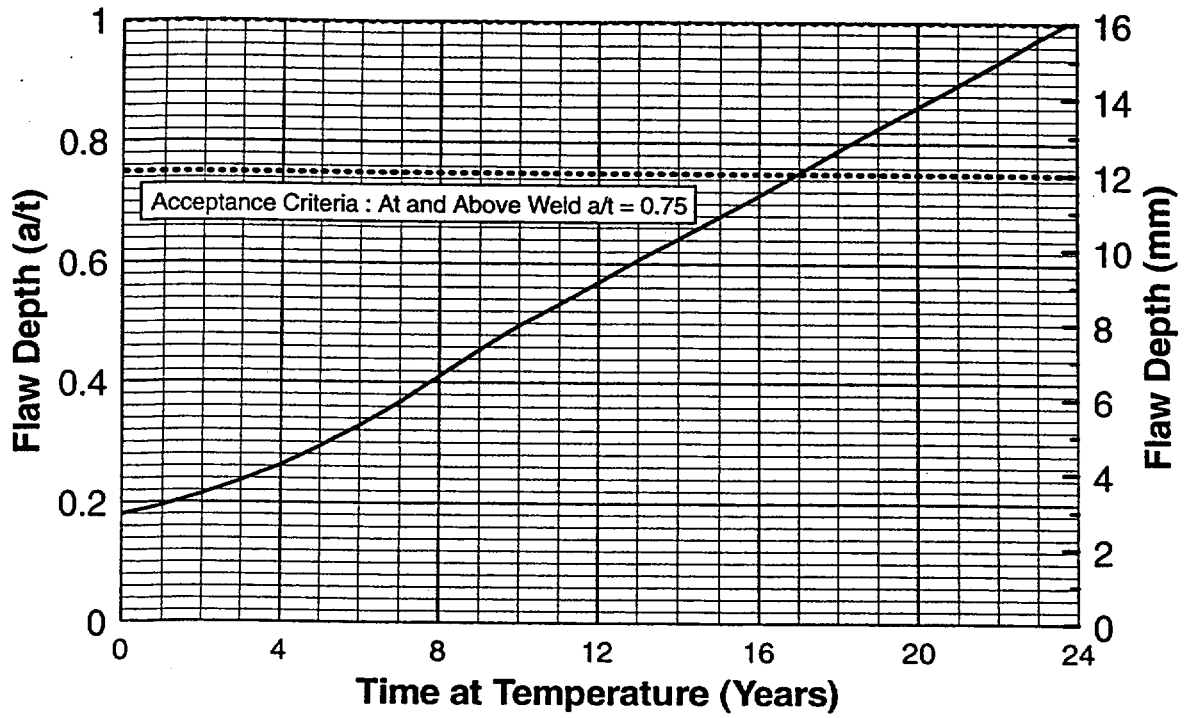

FIGURE 6-1b

CRACK GROWTH PREDICTIONS FOR LONGITUDINAL INSIDE SURFACE FLAWS IN THE HEAD PENETRATIONS AT THE NORTH ANNA AND SURRY UNITS, ABOVE THE ATTACHMENT WELD

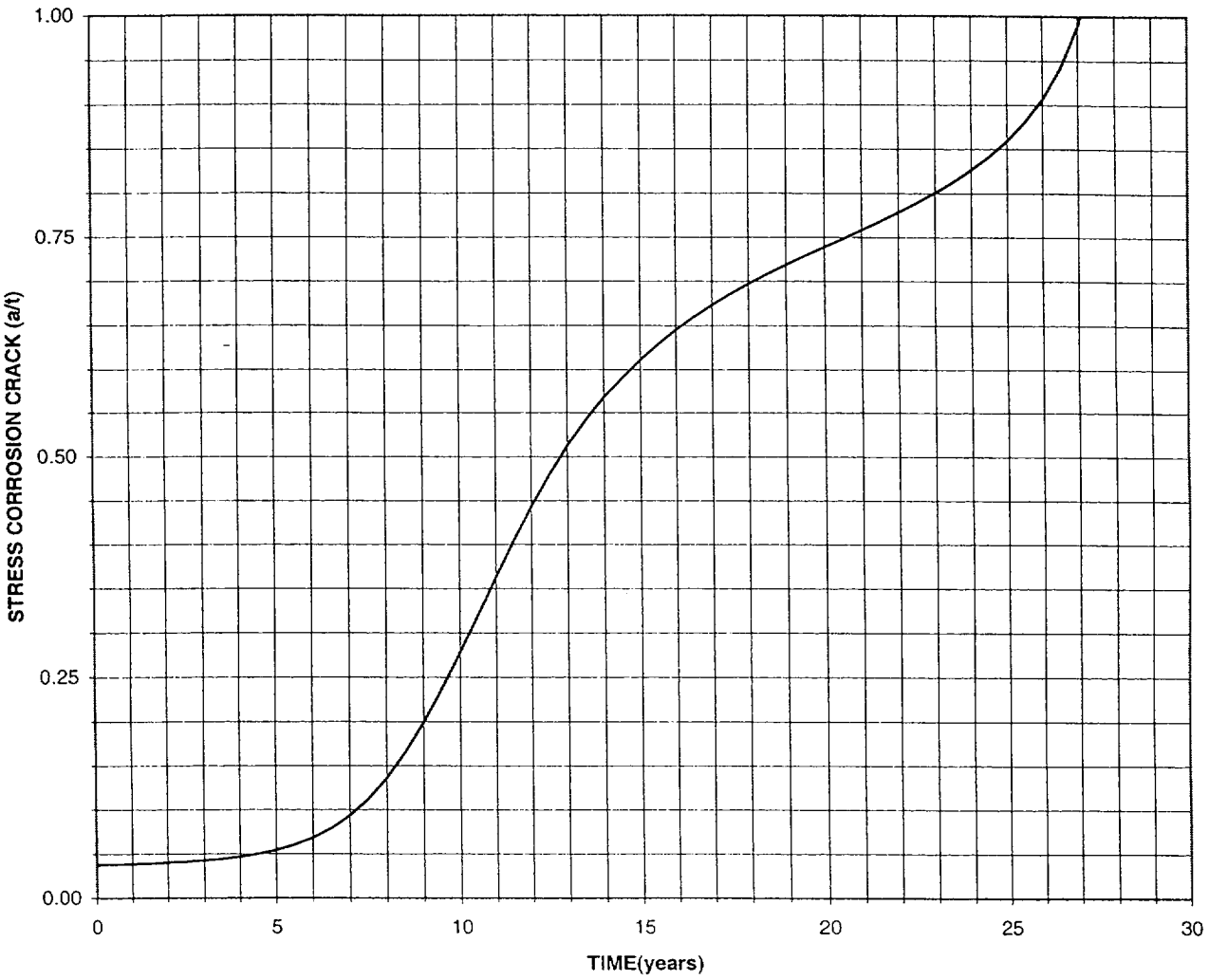

FIGURE 6-1c

CRACK GROWTH PREDICTIONS FOR LONGITUDINAL OUTSIDE SURFACE FLAWS IN THE HEAD PENETRATIONS AT THE NORTH ANNA AND SURRY UNITS

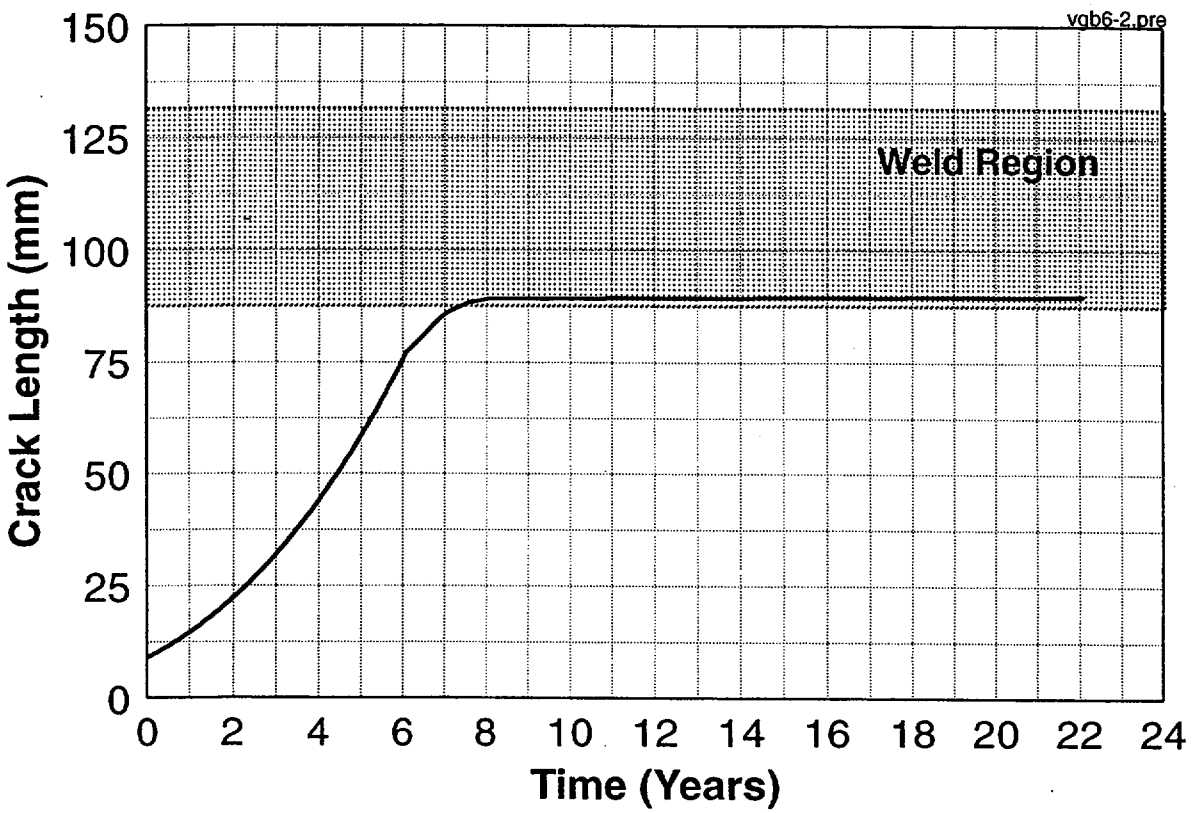

FIGURE 6-2

CRACK GROWTH PREDICTIONS FOR THROUGH-WALL FLAWS LOCATED AT THE LOWER HILLSIDE IN THE OUTERMOST HEAD PENETRATIONS OF NORTH ANNA AND SURRY UNITS

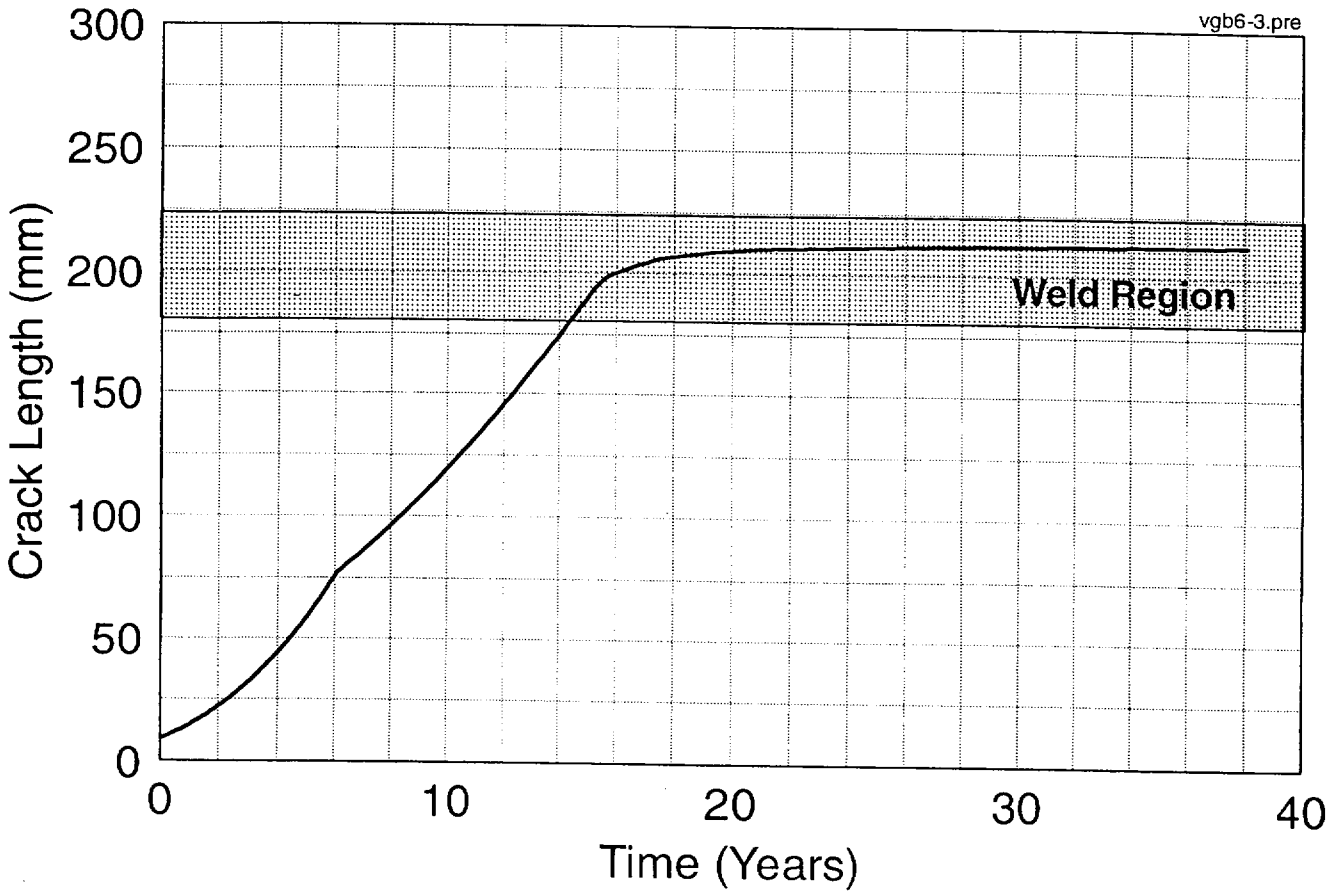

FIGURE 6-3

CRACK GROWTH PREDICTIONS FOR THROUGH-WALL FLAWS LOCATED AT THE CENTER SIDE OF THE OUTERMOST HEAD PENETRATIONS OF NORTH ANNA AND SURRY UNITS

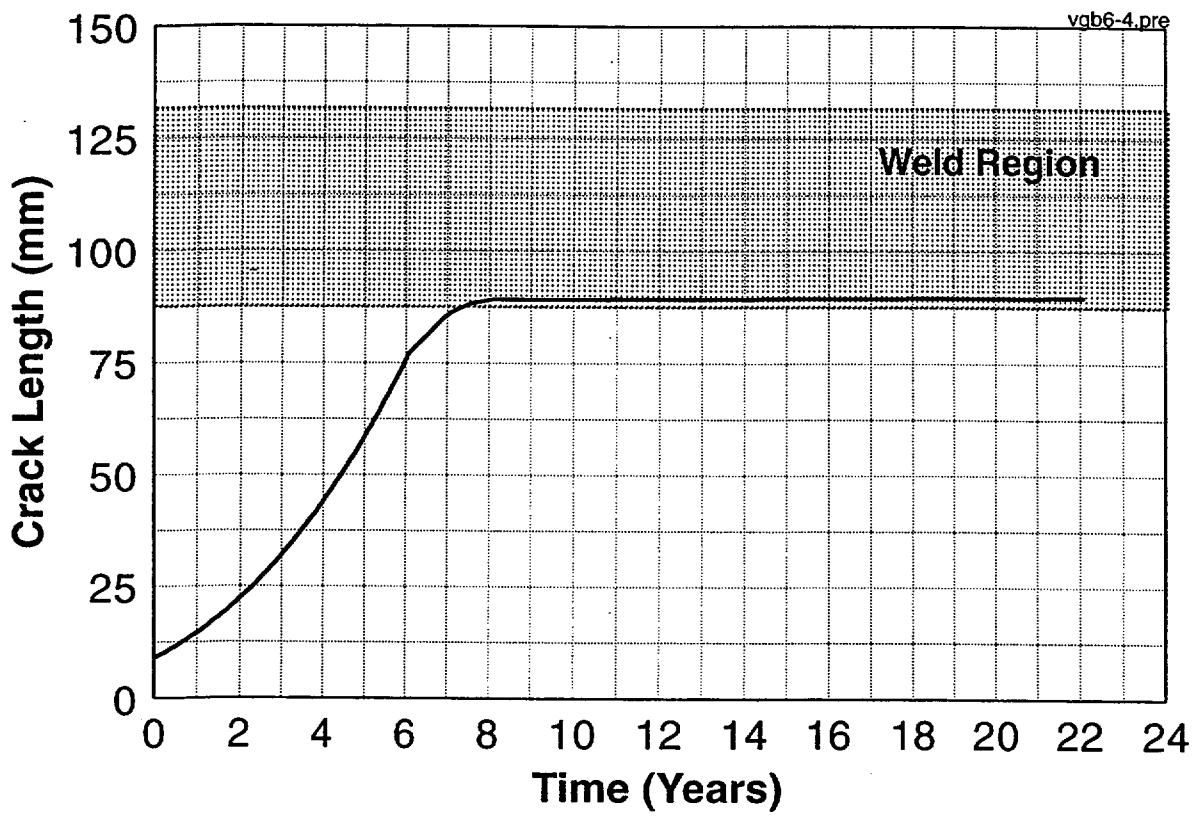

FIGURE 6-4

CRACK GROWTH PREDICTIONS FOR THROUGH-WALL FLAWS LOCATED AT THE LOWER HILLSIDE IN THE NEXT OUTERMOST HEAD PENETRATIONS OF NORTH ANNA AND SURRY UNITS

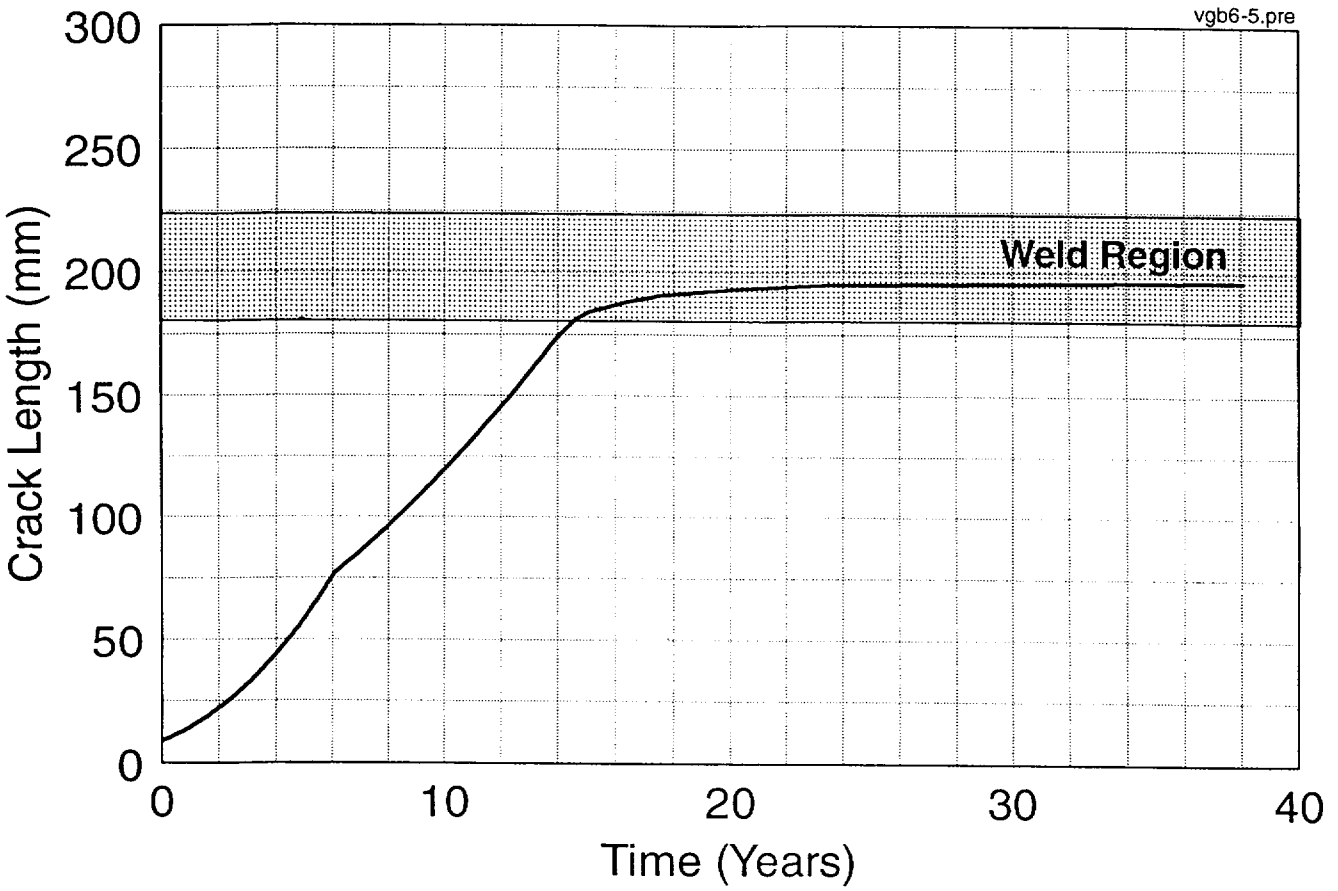

FIGURE 6-5

CRACK GROWTH PREDICTIONS FOR THROUGH-WALL FLAWS LOCATED AT THE CENTER SIDE OF THE NEXT OUTERMOST HEAD PENETRATIONS OF NORTH ANNA AND SURRY UNITS

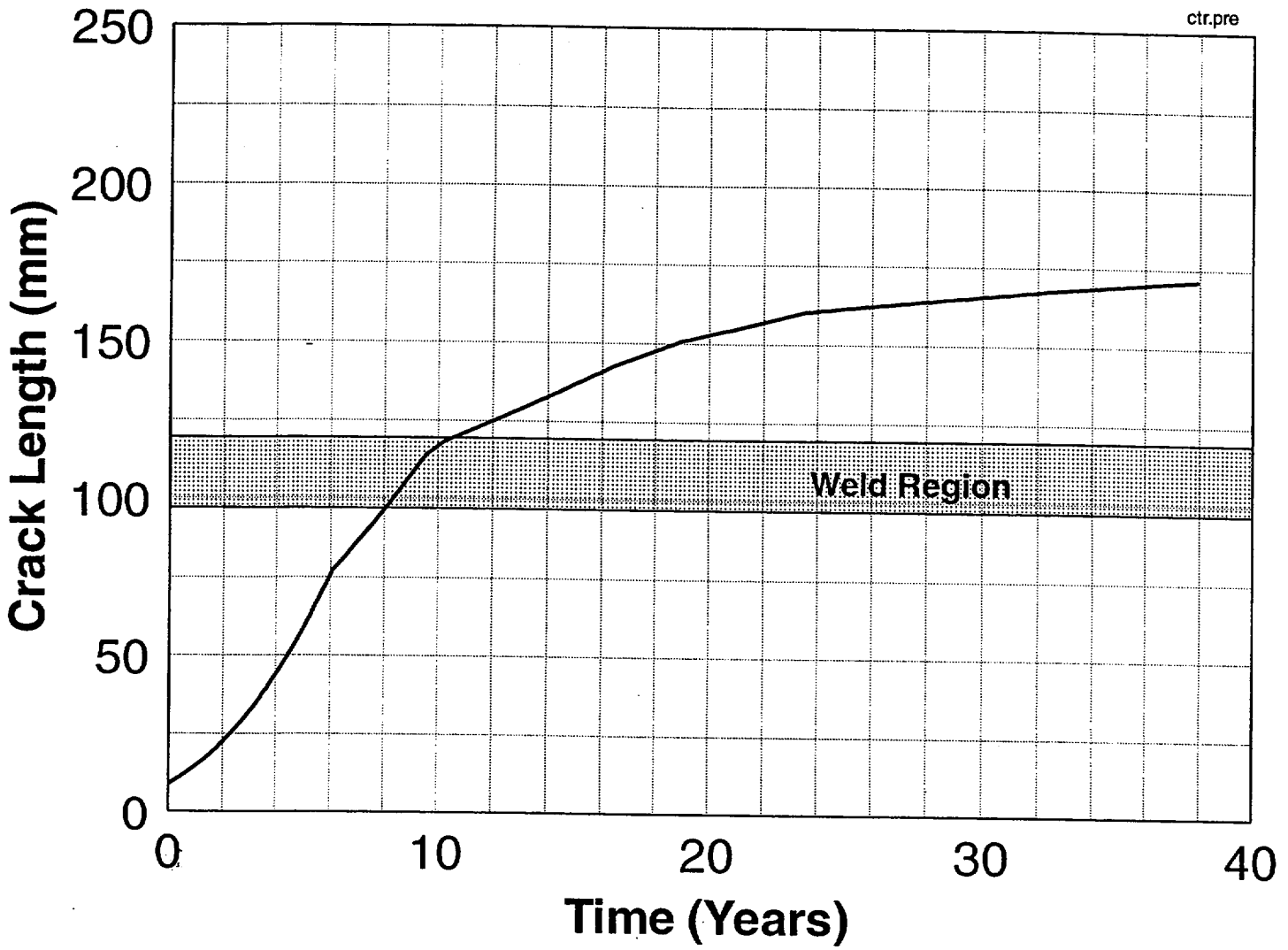

FIGURE 6-6

CRACK GROWTH PREDICTIONS FOR GROWTH OF THROUGH-WALL FLAWS IN THE CENTER PENETRATION AT THE NORTH ANNA AND SURRY UNITS

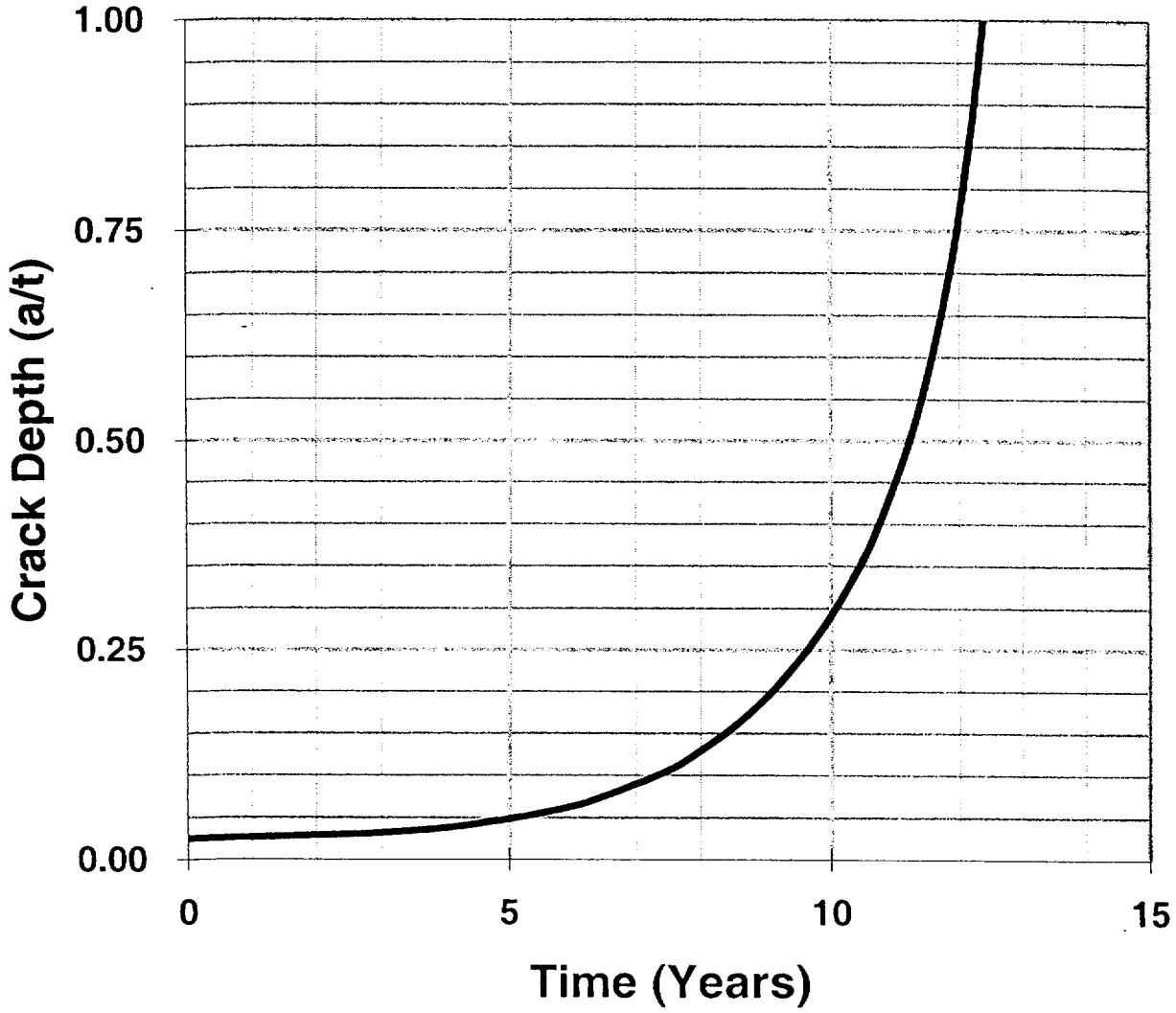

FIGURE 6-7

CRACK GROWTH PREDICTIONS FOR CIRCUMFERENTIAL SURFACE FLAWS NEAR THE TOP OF THE ATTACHMENT WELD

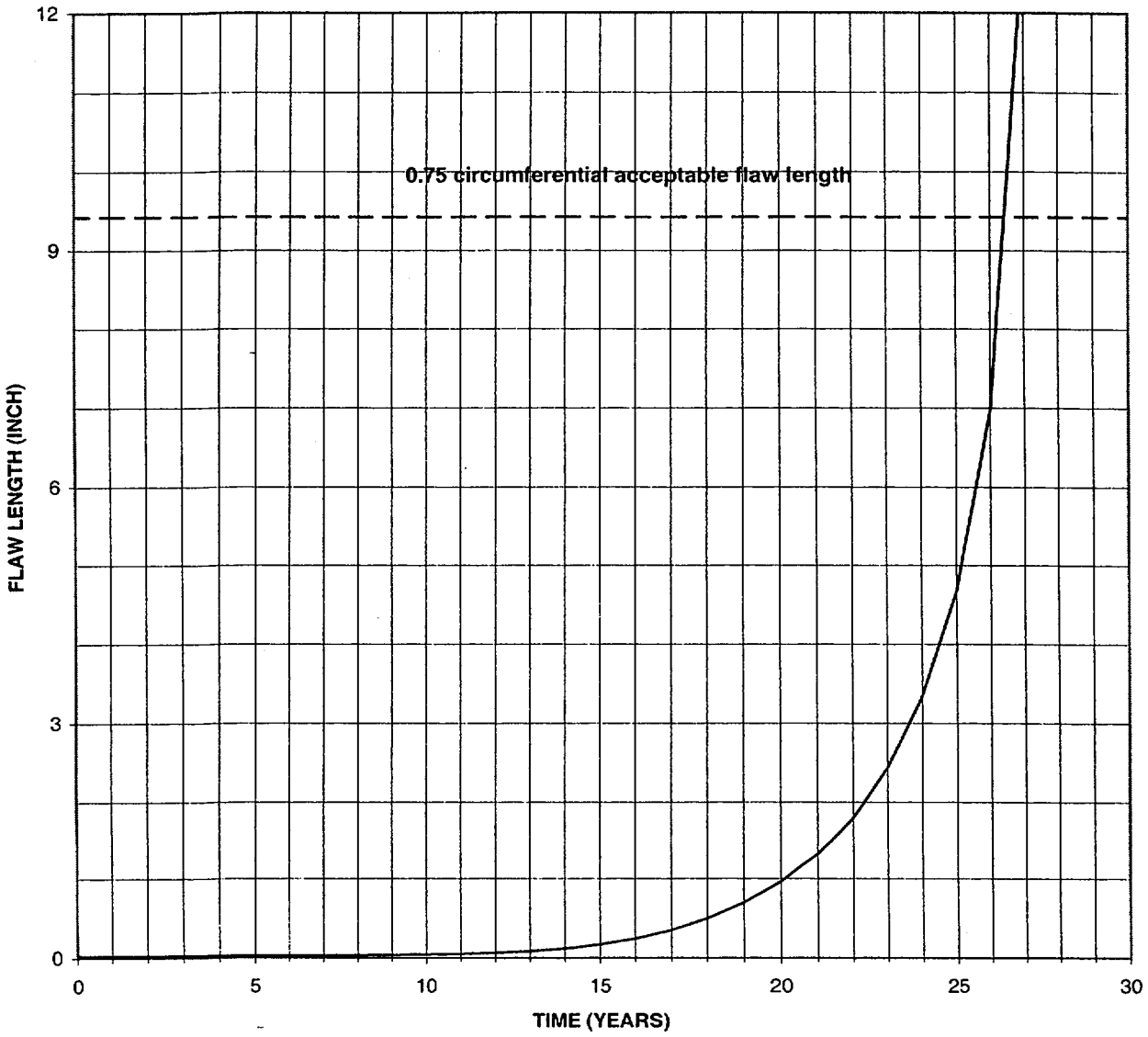

FIGURE 6-8

CRACK GROWTH PREDICTIONS FOR CIRCUMFERENTIAL THROUGH-WALL CRACKS NEAR THE TOP OF THE ATTACHMENT WELD

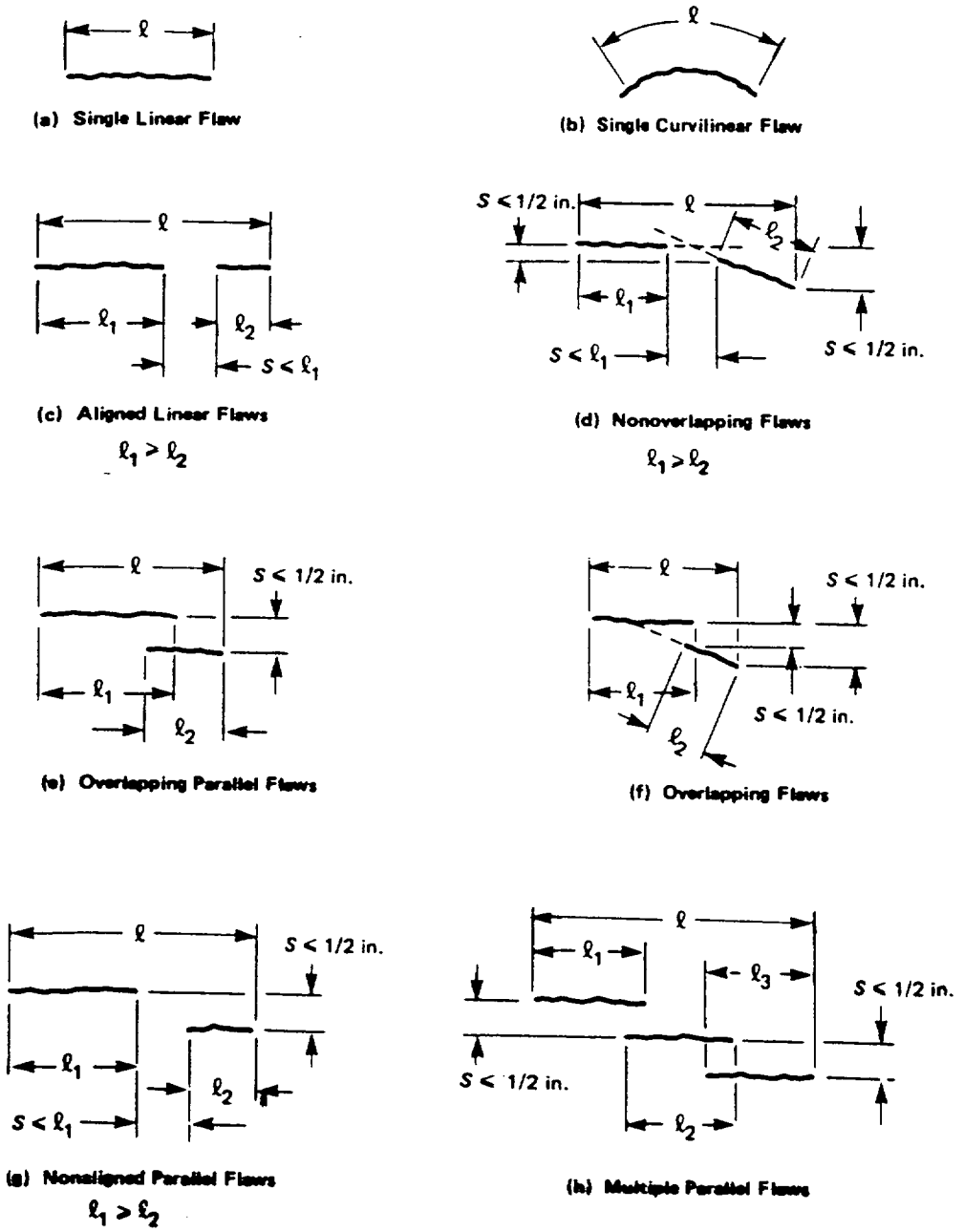

FIGURE 6-9

SECTION XI FLAW PROXIMITY RULES (FIGURE IWA-3400-1)

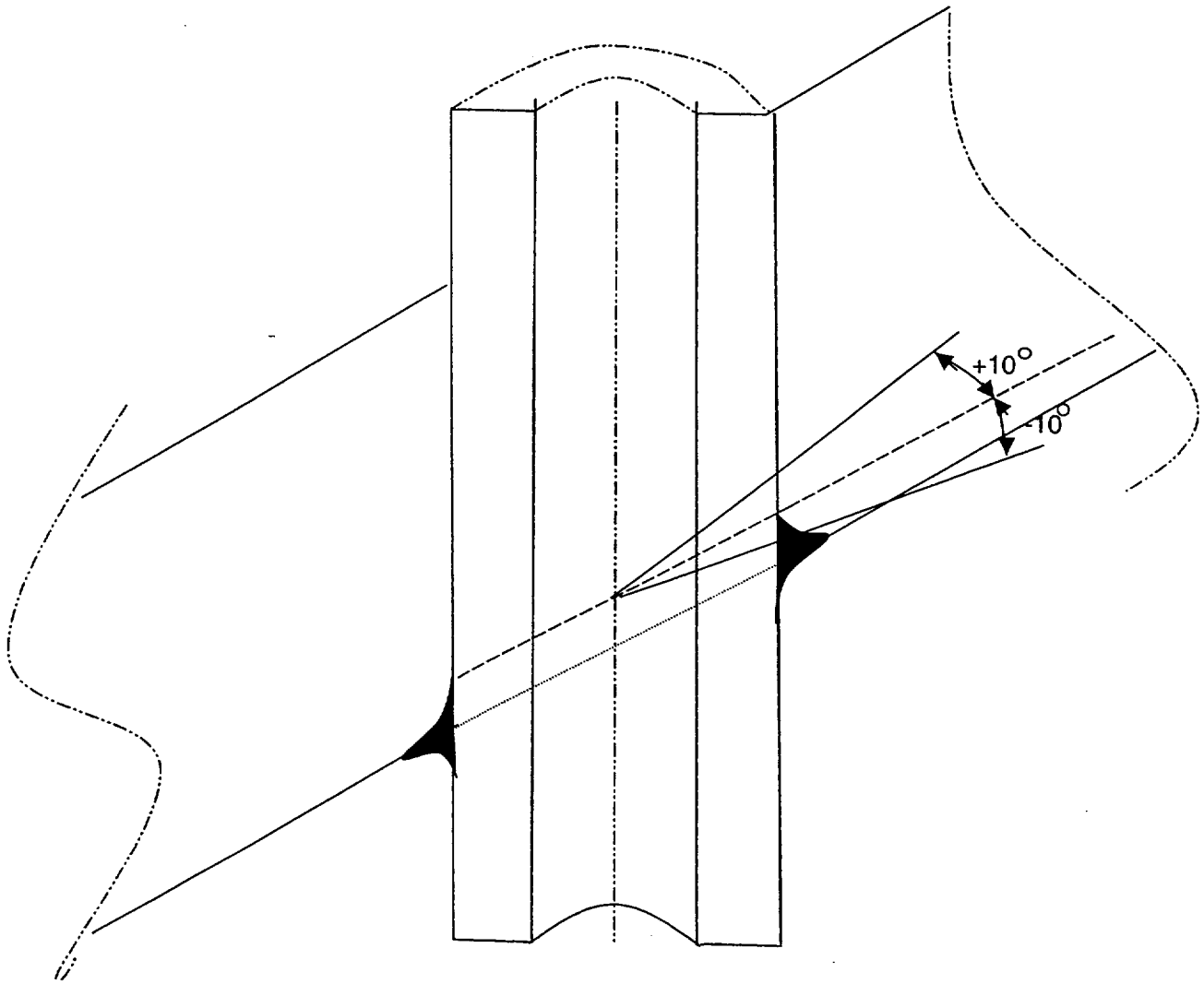

FIGURE 6-10

DEFINITION OF "CIRCUMFERENTIAL"

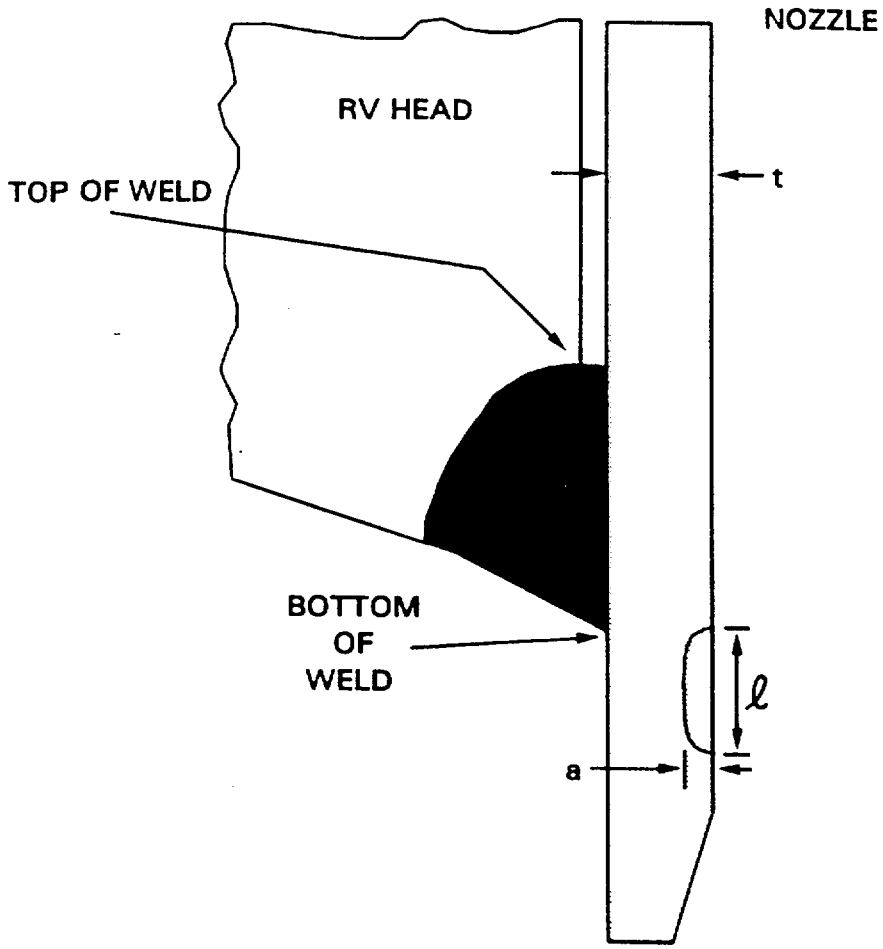

FIGURE 6-11

SCHEMATIC OF HEAD PENETRATION GEOMETRY

SECTION 7.0
FLAW DISPOSITION STRATEGIES

In the event that one or more flaws are discovered during inspections of the Surry or North Anna Units, a number of options have been developed. The choice of a particular option is dependent on the size and location of the flaw, as well as the time remaining in the outage.

There are many possible options, but at present Virginia Power has chosen to develop three to a mature state, ready for use immediately if needed. Each of these options is described below.

1. Disposition by flaw evaluation. If the flaw can be shown to be in compliance with the industry flaw acceptance criteria for a period of time, the flaw is acceptable for service during that period. See Section 6 flaw evaluation charts.

2. Repair by excavation. Electrical discharge machining can be used to remove the flaw. The maximum depth of excavation depends on the location, and the technical basis for the maximum excavation depth is contained in Reference 11.

3. Repair by partial excavation and weld overlay at the inside surface, or simply overlay at the outside surface or over the attachment weld to seal the remaining flaw from the water environment (embedded flaw repair). A sketch showing the approach schematically appears as Figure 7-1.

These options each have advantages and disadvantages. The flaw evaluation option is the fastest disposition, but the flaw may continue to propagate and will require additional inspection and eventual repair. The flaw excavation option is the fastest repair but is limited in application due to access, and follow-up inspections are more difficult. The weld overlay repair requires more time, but permanently seals the flaw from the environment, and leaves a surface which allows for follow-up inspections if necessary.

7.1 AXIAL FLAWS IN THE PENETRATION TUBE AT AND ABOVE WELD

The disposition strategies for this situation are shown in Table 7-1. It can be seen from this table that in many cases there are a number of viable options. Footnotes in the table point out the restrictions and possible concerns with the options specified.

Penetrations Without a Thermal Sleeve. Five possible scenarios exist, depending on the flaw depth relative to the acceptance limit and the excavation limit. The strategies have been developed for use at any time. For example, if a flaw is found which has a depth less than the acceptance limit, options should be considered for its presently existing depth as well as its predicted depth after the next fuel cycle. The maximum acceptance limits for flaws as well as the maximum excavation limits are shown in Figure 7-2. The crack depth at some future time can be estimated using the flaw charts of Section 6.

If a flaw is discovered whose depth is less than the acceptance limit, all three options are available, unless the depth is greater than the excavation limit.

If the flaw depth exceeds the acceptance limit, it must be repaired, and as long as it is within the excavation limit, both repair options are available. For deep flaws, the embedded flaw repair option is the only one available.

Penetrations With a Thermal Sleeve. For these penetrations, the maximum excavation depth is more restricted, because of the smaller area inside the thermal sleeve to fit tooling, and because of the restrictions involved in doing an excavation through a window in the thermal sleeve. Again the strategies apply for any time frame, whether it be the present time, or some time in the future. The maximum acceptance limits for flaws as well as the maximum excavation limits are shown in Figure 7-3. The future depth of a flaw can be predicted using the flaw charts of Section 6.

If a flaw is discovered whose depth is less than the flaw acceptance limit, all options are available, as long as the flaw is relatively shallow (0.25 inch or less). The excavation limit is relatively small for the sleeved penetrations, because of the necessity to do the excavation through a window in the thermal sleeve.

If the flaw depth exceeds the acceptance limit, it must be repaired, and for sleeved penetrations this generally means that the only viable option is the embedded flaw repair, which can be carried out through a window in the thermal sleeve.

7.2 AXIAL FLAWS IN THE PENETRATION TUBE BELOW THE WELD

Disposition of flaws which are located below the weld is much easier, because the flaw acceptance limits are more liberal. The flaw is allowed to extend completely through the penetration wall, as long as its upper extremity is a sufficient distance below the bottom of the weld. The strategies for flaws below the

weld are shown in Table 7-2, and are dependent upon the distance from the upper extremity of the flaw to the bottom of the weld. The predicted future flaw growth is a key element in this strategy, and these predictions can be obtained from the flaw charts in Section 6.

Penetrations Without a Thermal Sleeve. The flaw can be left as is, with no repair required, as long as the distance from the upper extremity of the flaw to the bottom of the weld is greater than the predicted growth of the flaw in length. Excavation or embedded flaw weld overlay repair remain options regardless of the depth of the flaw, as long as its upper extremity remains below the bottom of the weld.

Penetrations With a Thermal Sleeve. As is the case without a thermal sleeve, a flaw can be left in the penetration with no repair required, as long as its upper extremity is predicted to remain below the bottom of the weld. The repair options in this case are somewhat more limited, because of restrictions on the depth of excavation through a window in the thermal sleeve. In all cases, the embedded flaw weld overlay is an option.

7.3 FLAWS IN THE ATTACHMENT WELD

Since flaws in this region cannot be accepted by analysis, repair is the only option here. Flaw excavation or the embedded flaw repair are both possible, but the embedded flaw technique is the only one which can presently be performed remotely.

7.4 CIRCUMFERENTIAL FLAWS ABOVE THE ATTACHMENT WELD

This type of flaw clearly has the potential to pose a safety risk, and therefore must be dealt with on a case by case basis. The most likely disposition of such a flaw would be by repair using the embedded flaw repair. It is also possible to remove the flaw by progressive grinding or electrical discharge machining (EDM), and then rewelding to the original configuration.

TABLE 7-1
REPAIR OPTIONS - AXIAL FLAWS AT OR ABOVE THE ATTACHMENT WELD

Penetration Type	AXIAL Flaw Depth	Leave As Is	Excavate	Excavate & Weld Overlay Of Embedded Flaw
Without Thermal Sleeve	< Flaw Accept. Limit & < Excavation Limit	X	X[1]	X[2]
	< Flaw Accept. Limit & > Excavation Limit	X	NA	X[2]
	> Flaw Accept. Limit & < Excavation Limit	NA	X[1]	X[2]
	> Flaw Accept. Limit & > Excavation Limit	NA	NA	X[2]
	> 12 mm	NA	NA	X[4]
With Thermal Sleeve	< Flaw Accept. Limit & < 6.35 mm	X	X[1,3]	X[2,3]
	< Flaw Accept. Limit & > 6.35 mm	X	NA	X[2,3]
	> Flaw Accept. Limit & > 6.35 mm	NA	NA	X[2,3]
	> 12 mm	NA	NA	X[2,4]

DEFINITIONS: NA = Not Applicable

NOTES:
1) Restricts reinspection techniques
2) Non Section XI repair, as approved by NRC [12]
3) Requires window in thermal sleeve
4) Requires NRC approval of ASME Code relief for weld overlay of embedded flaw for flaws > .75 wall thickness (12 mm)

TABLE 7-2
REPAIR OPTIONS - AXIAL FLAWS BELOW THE ATTACHMENT WELD

Penetration Type	AXIAL Flaw Depth	Distance From Upper Extremity Of Flaw To Bottom Of Weld	Leave As Is	Excavate	Excavate & Weld Overlay Of Embedded Flaw
Without Thermal Sleeve	< through wall projected after 1 cycle	> Predicted Growth	X	X[1]	X[2]
		< Predicted Growth	NA	X[1]	X[2]
	through wall	> Predicted Growth	X	X[4]	X[4]
		< Predicted Growth	NA	X[4]	X[4]
With Thermal Sleeve	< through wall projected after 1 cycle & < 6.35 mm	> Predicted Growth	X	X[1,3]	X[2,3]
		< Predicted Growth	NA	X[1,3]	X[2,3]
	< through wall projected after 1 cycle & > 6.35 mm	> Predicted Growth	X	NA	X[2,3]
		< Predicted Growth	NA	NA	X[2,3]
	through wall	> Predicted Growth	X	NA	X[3,4]
		< Predicted Growth	NA	NA	X[3,4]

DEFINITIONS: NA = Not Applicable

NOTES:
1) Restricts reinspection techniques
2) Non Section XI repair, as approved by NRC [12]
3) Requires window in thermal sleeve
4) Requires NRC approval of ASME Code relief for weld overlay or excavation for flaws > .75 wall thickness (12 mm)

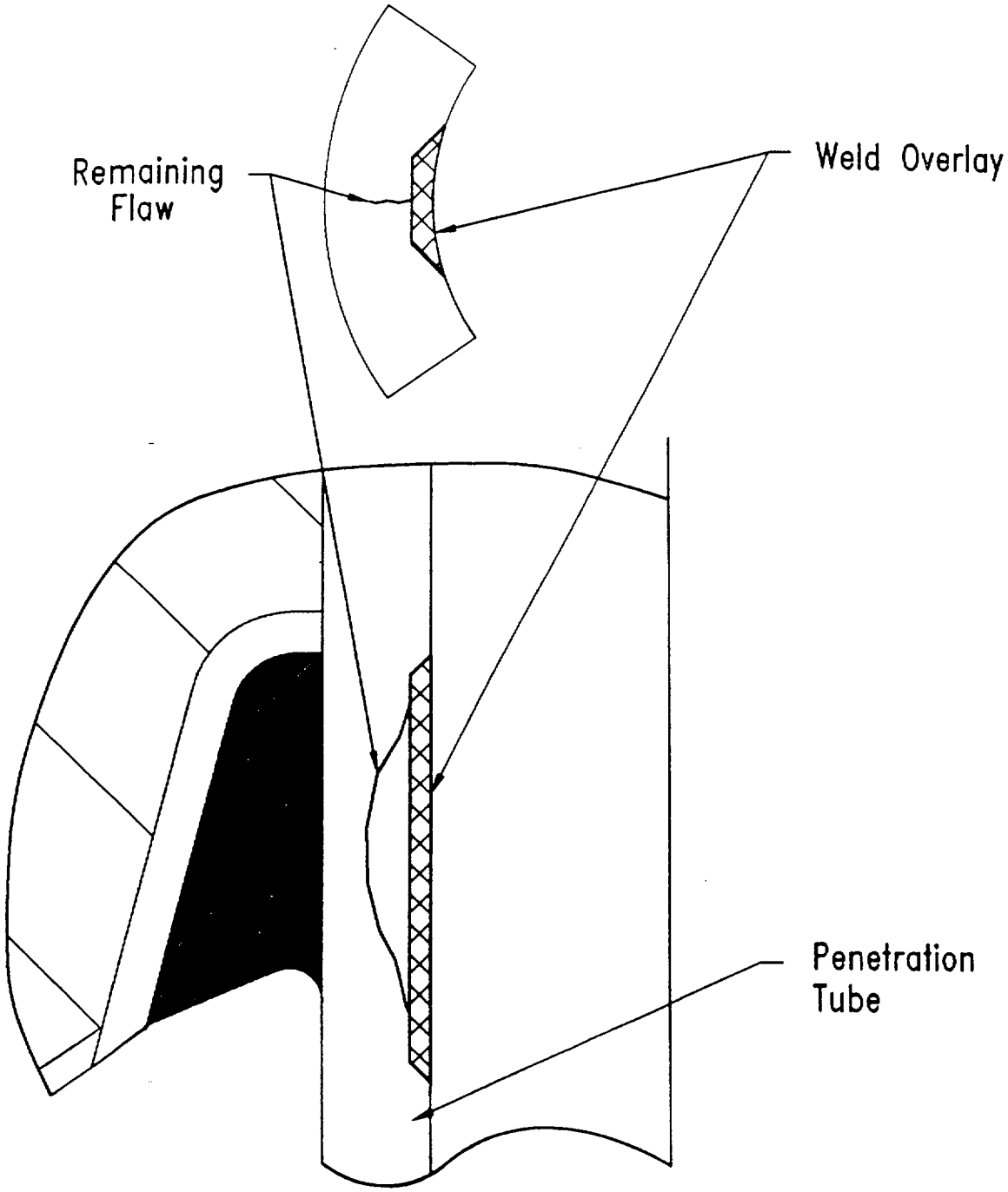

FIGURE 7-1
SCHEMATIC OF EMBEDDED FLAW REPAIR

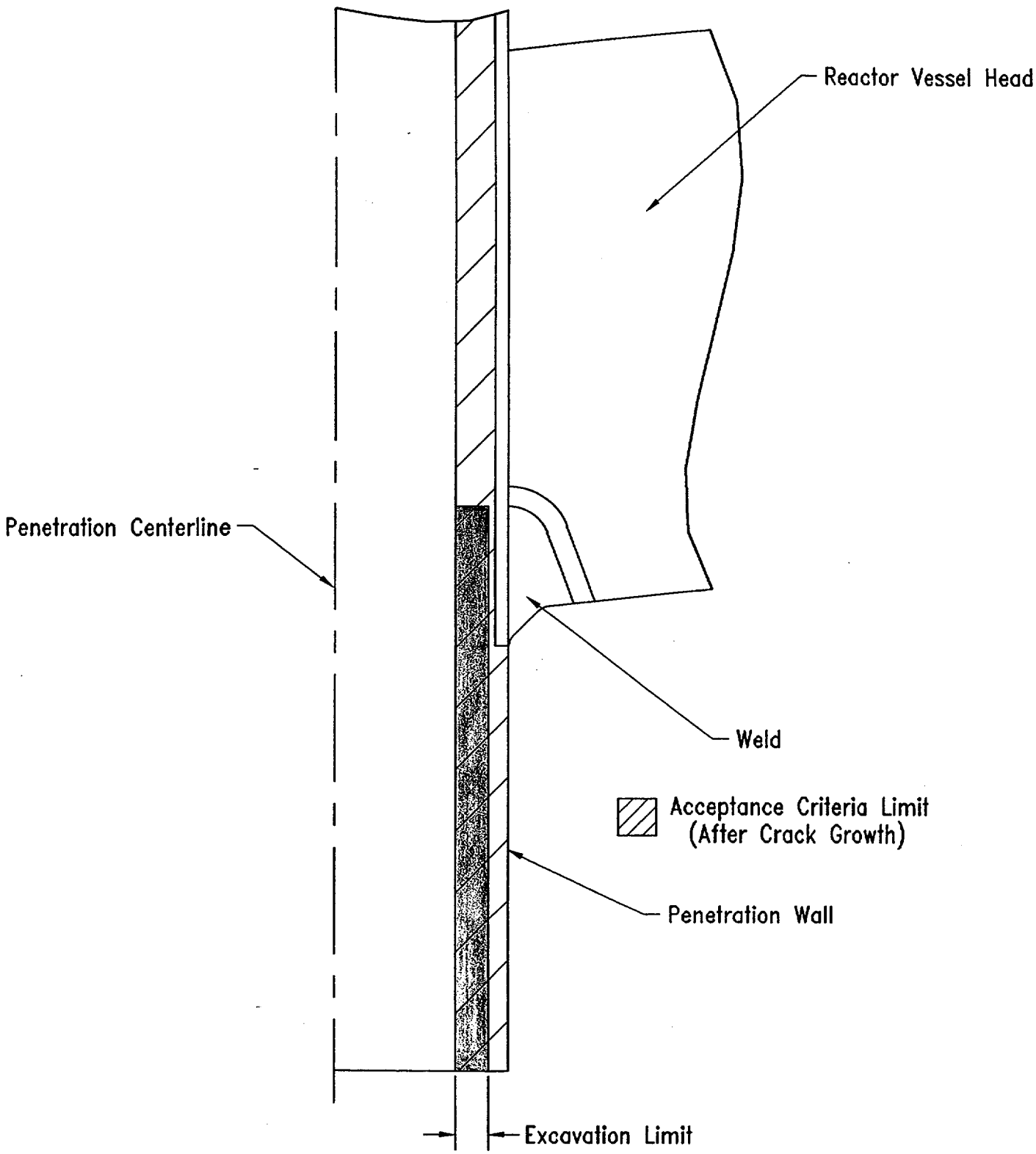

FIGURE 7-2
MAXIMUM FLAW ACCEPTANCE AND EXCAVATION LIMITS FOR
PENETRATIONS WITH NO THERMAL SLEEVE

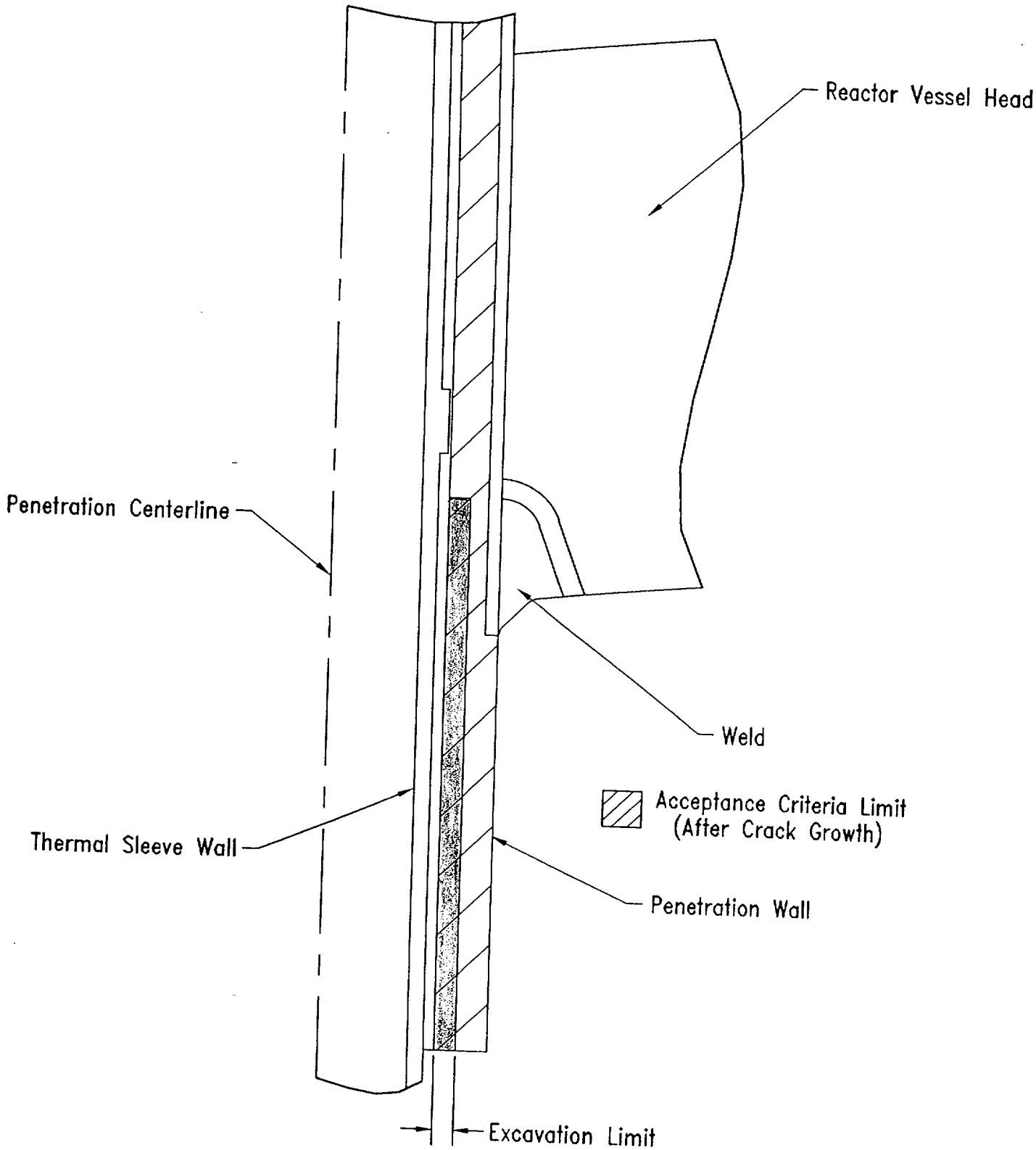

FIGURE 7-3
MAXIMUM FLAW ACCEPTANCE AND EXCAVATION LIMITS FOR
PENETRATIONS WITH THERMAL SLEEVES

SECTION 8.0
SUMMARY AND CONCLUSIONS

An extensive evaluation has been carried out to characterize the loadings and stresses which exist in the head penetrations at the North Anna and Surry Units. Three-dimensional finite element models were used, and all pertinent loadings on the penetrations were analyzed[6]. These loadings included internal pressure and thermal expansion effects typical of steady state operation. In addition, residual stresses due to the welding of the penetrations to the vessel head were considered.

Results of the analyses reported here are consistent with the axial orientation and location of flaws which have been found in service in a number of plants, in that the largest stress component is the hoop stress, and the maximum stresses were found to exist in the circumferential locations nearest and farthest away from the center of the head. The most important loading conditions were found to be those which exist on the penetration for the majority of the time, which are the steady state loading and the residual stresses.

These stresses are important because the cracking observed to date in operating plants has been determined to result from primary water stress corrosion cracking (PWSCC). These stresses were used in fracture calculations to predict the future growth of flaws postulated in the head penetrations. A crack growth law was developed specifically for the operating temperature of the head at the North Anna and Surry Units, based on information from the literature as well as a compilation of crack growth results for operating plants.

The crack growth predictions contained in Section 6 show that the future growth of cracks which might be found in the penetrations will be very slow, and that a number of effective full power years will be required for any significant extensions.

Safety Assessment

It is appropriate to examine the safety consequences of an indication which might be found. The indication, even if it were to propagate through the penetration wall, would have only minor consequences, since the pressure boundary would not be broken, unless it were to propagate above the weld.

Further propagation of the indication would not change its orientation, since the hoop stresses in the penetration are much larger than the axial stresses. Therefore, it is extremely unlikely that the head penetration would be severed as a result of any indications.

If the indication were to propagate above the weld, a leak could result, but the magnitude of such a leak would be very small, because the crack could not open significantly due to the tight fit between the penetration and the vessel head. Such a leak would have no immediate impact on the structural integrity

of the system, but could lead to wastage in the ferritic steel of the vessel head, as the borated primary water concentrates due to evaporation.

Any indication is unlikely to propagate very far up the penetration above the weld, because the hoop stresses decrease in this direction, and this will cause it to slow down, and to stop before it reaches the outside surface of the head. This result supports the conclusion that it is extremely unlikely that leakage of any magnitude will occur.

The high likelihood that the indication will not propagate beyond the head ensures that no catastrophic failure of the head penetration will occur, since the indication will be enveloped in the head itself, which precludes the opening of the crack and limits leakage.

SECTION 9
REFERENCES

1. Scott, P. M., "An Analysis of Primary Water Stress Corrosion Cracking in PWR Steam Generators," in Proceedings, Specialists Meeting on Operating Experience With Steam Generators, Brussels Belgium, Sept. 1991, pages 5, 6.

2. McIlree, A. R., Rebak, R. B., Smialowska, S., "Relationship of Stress Intensity to Crack Growth Rate of Alloy 600 in Primary Water," Proceedings International Symposium Fontevraud II, Vol. 1, p. 258-267, September 10-14, 1990.

3. Cassagne, T., Gelpi, A., "Measurements of Crack Propagation Rates on Alloy 600 Tubes in PWR Primary Water," in Proceedings of the 5th International Symposium on Environmental Degradation of Materials in Nuclear Power Systems-Water Reactors," August 25-29, 1991, Monterey, California.

4. Bamford, W. H., and Foster, J. P., "Crack Growth and Microstructural Characterization of Alloy 600 PWR Vessel Head Penetration Materials," EPRI Report TR 109136 Final Report, December 1997.

5A. McGowan, J. J. and Raymund, M., "Stress Intensity Factor Solutions for Internal Longitudinal Semi-elliptic Surface Flaw in a Cylinder Under Arbitrary Loading," ASTM STP 677, 1979, pp. 365-380.

5B. Newman, J. C. and Raju, I. S., "Stress Intensity Factor Influence Coefficients for Internal and External Surface Cracks in Cylindrical Vessels," in Aspects of Fracture Mechanics in Pressure Vessels and Piping, PVP Vol. 58, ASME, 1982, pp. 37-48.

6. [

]a,c,e

7. USNRC Letter, W. T. Russell to W. Raisin, NUMARC, "Safety Evaluation for Potential Reactor Vessel Head Adapter Tube Cracking," November 19, 1993.

8. USNRC Letter, A. G. Hansen to R. E. Link, "Acceptance Criteria for Control Rod Drive Mechanism Penetrations at Point Beach Nuclear Plant, Unit 1," March 9, 1994.

9. Letter from G. L. Darden to R. W. Calder, Virginia Power, "Reactor Vessel Coolant Temperature Design Input for Use in North Anna Units 1 and 2 Upper Head Penetration Inspection Program," Letter No. NAF-95-129, October 4, 1995.

10. Letter from G. M. Suwal to R. W. Calder, Virginia Power, "Reactor Coolant Temperature Design Input for Use in Surry Units 1 and 2 Upper Head Penetration Inspection Program," Letter No. NAF-95-162, November 27, 1995.

11. Yu, C., Butler, T., "Determination of Maximum Excavation Depth on Reactor Head Penetrations for North Anna Unit 1," Westinghouse Electric WCAP-14562, January 1996.

12. USNRC Letter, David B. Matthews to J. P. O'Hanlon, "North Anna Unit 1 – Use of an Alternative Repair Technique for Reactor Vessel Head Penetrations," February 5, 1996.

13. Virginia Electric and Power Co. Response to NRC Bulletin 2001-01, Circumferential Cracking of Reactor Vessel Head Penetration Nozzles, Docket Nos. 50-338/339 and 50-280/281, dated August 31, 2001.

APPENDIX A
ALLOWABLE AREAS OF LACK OF FUSION: WELD FUSION ZONES

There are two fusion zones of interest for the head penetration attachment welds, the penetration itself (Alloy 600) and the reactor vessel head material (A533B ferritic steel). The operating temperature of the upper head region of the North Anna and Surry Units is 318°C (604°F), so both materials will be very ductile. The toughness of both materials is quite high, so any flaw propagation along either of the fusion zones will be totally ductile.

Two calculations were completed for the fusion zones, one for the critical flaw size, and the second for the allowable flaw size, which includes the margins required in the ASME code. The simpler case is the Alloy 600 fusion zone, where the potential failure will be a pure shearing of the penetration as the pressurized penetration tube is forced outward from the vessel head, as shown in Figure A-1.

The failure criterion will be that the average shear stress along the fusion line exceeds the limit shear stress. For the critical flaw size, the limiting shear stress is the shear flow stress, which is equal to half the tensile flow stress, according to the Tresca criterion. The tensile flow stress is the average of the yield stress and ultimate tensile stress of the material. The criterion for Alloy 600 at 318°C (604°F) is:

$$\text{Average shear stress} < \text{shear flow stress} = 26.85 \text{ ksi}$$

This value was taken from the ASME Code, Section III, Appendix I, at 600°F.

For each penetration, the axial force which produces this shear stress results from the internal pressure. Since each penetration has the same outer diameter, the axial force is the same. The average shear stress increases as the load carrying area decreases (the area of lack of fusion increases). When this increasing lack of fusion area increases the stress to the point at which it equals the flow stress, failure occurs. This point may be termed the critical flaw size. This criterion is actually somewhat conservative. Alternatively, use of the Von Mises failure criterion would have set the shear flow stress equal to 60 percent of the axial flow stress, and would therefore have resulted in larger critical flaw sizes.

The allowable flaw size, as opposed to the critical flaw size discussed above, was calculated using the allowable limit of Section III of the ASME Code, paragraph NB 3227.2. The criterion for allowable shear stress then becomes:

$$\text{Average shear stress} < 0.6\ S_m = 13.98\ \text{ksi}$$

where S_m = the ASME Code limiting design stress from Section III, Appendix I.

The above approach was used to calculate the allowable flaw size and critical flaw size for the outermost and center penetrations. The results show that a very large area of lack of fusion can be tolerated by the head penetrations, regardless of their orientation. These results can be illustrated for the outermost presentation.

The total surface contact area for the fusion zone on the outermost head penetration is 17.4 in^2. The calculations above result in a required area to avoid failure of only 1.45 in^2, and using the ASME Code criteria, the area required is 2.79 in^2. These calculations show that as much as 83.9 percent of the weld may be unfused, and the code acceptance criteria can still be met.

To envision the extent of lack of fusion which is allowable, Figure A-2 was prepared. In this figure, the weld fusion region for the outermost penetration has been shown in an unwrapped, or developed view. The figure shows the extent of lack of fusion which is allowed, in terms of limiting lengths for a range of circumferential lack of fusion. This figure shows that the allowable vertical length of lack of fusion for a full circumferential unfused region is 84 percent of the weld length. Conversely, for a region of lack of fusion which extends the full vertical length of the weld, the circumferential extent is limited to 302 degrees. The extent of lack of fusion which would cause failure is labelled "critical" on this figure, and is even larger. The dimensions shown on this figure are based on an assumed rectangular area of lack of fusion.

The full extent of this allowable lack of fusion is shown in Figure A-3, where the axes have been expanded to show the full extent of the tube-weld fusion line. This figure shows that a very large area of lack of fusion is allowable for the outer most penetration. Similar results were found for the center penetration, where the weld fusion area is somewhat smaller at 16.1 in^2.

A similar calculation was also carried out for the fusion zone between the weld and the head, and the result is shown in Figure A-4. The allowable area of unfused weld for this location is 84.8 percent of the total area. This approach to the fusion zone with the carbon steel head is only approximate, but may provide a realistic estimate of the allowable. Note that even a complete lack of fusion in this region would not result in rod ejection, because the weld to the tube would prevent it.

The allowable lack of fusion for the weld fusion zone to the head may be somewhat in doubt, because of the different geometry, where one cannot ensure that the failure would be due to pure shear. To investigate this concern, additional finite element models were constructed with various degrees of lack of fusion discretely modelled, ranging from 30 to 65 percent. The stress intensities around the circumference of the penetration were calculated, to provide for the effects of all stresses, as opposed to the shear stress only, as used above. When the average stress intensity reaches the flow stress (53.7 ksi), failure is expected to occur. The code allowable stress intensity is 1.5 Sm, or 35 ksi, using the lower of the Alloy 600 and ferritic allowables at 316°C (600°F).

The results of this series of analyses are shown in Figure A-5, where it is clear that large areas of lack of fusion are allowable. As the area of lack of fusion increases, the stresses redistribute themselves, and the stress intensity does not increase in proportion to the area lost. These results seem to confirm that the shear stress is the only important stress governing the critical flaw size for the head fusion zone as well.

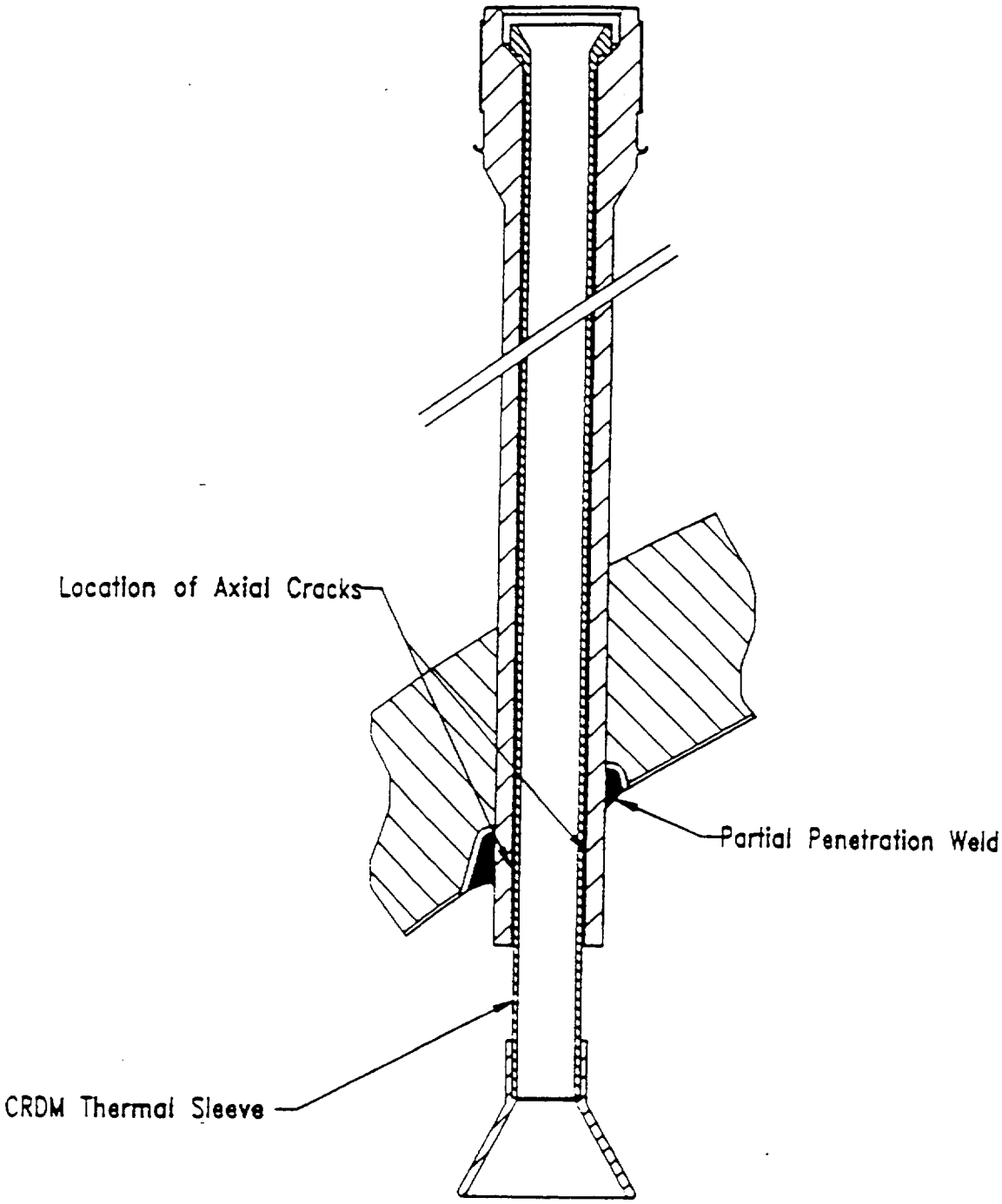

FIGURE A-1

TYPICAL HEAD PENETRATION

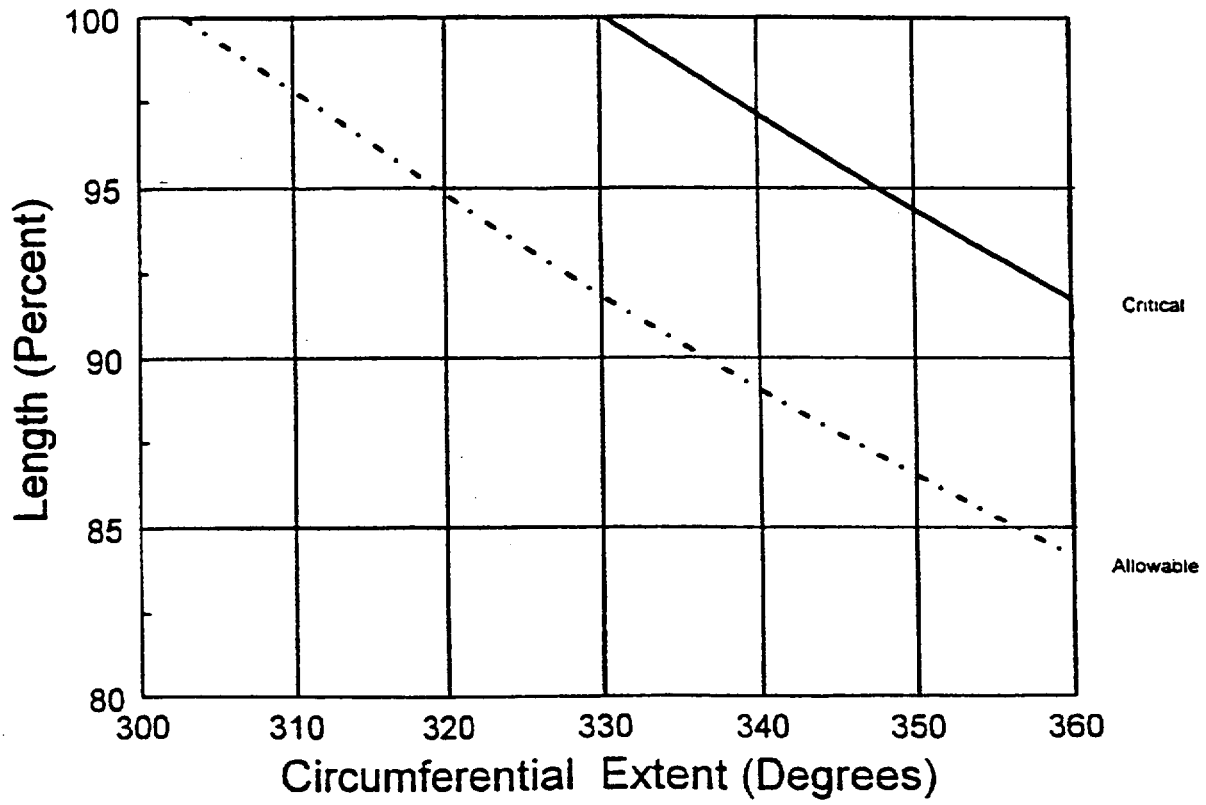

FIGURE A-2

ALLOWABLE REGIONS OF LACK OF FUSION FOR THE OUTMOST PENETRATION TUBE TO WELD FUSION ZONE: DETAILED VIEW

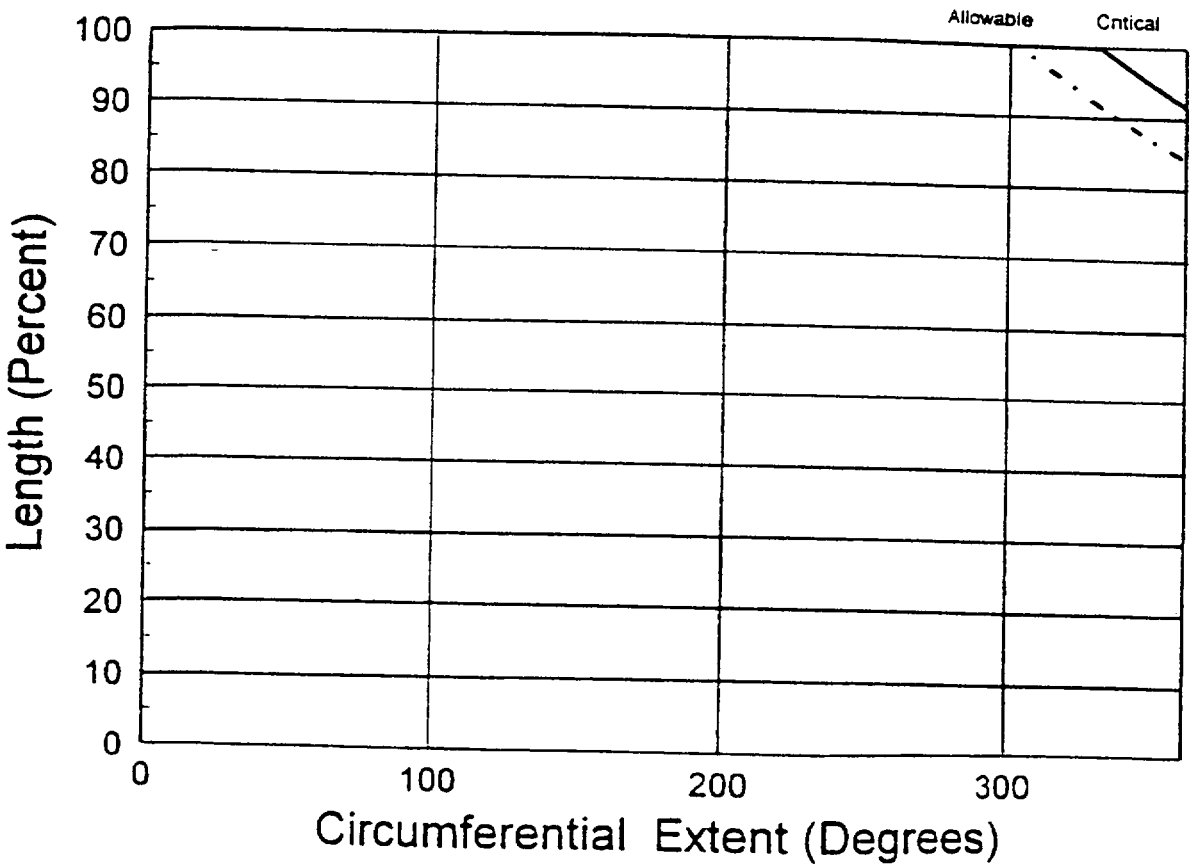

FIGURE A-3

ALLOWABLE REGIONS OF LACK OF FUSION FOR THE OUTERMOST PENETRATION TUBE TO WELD FUSION ZONE

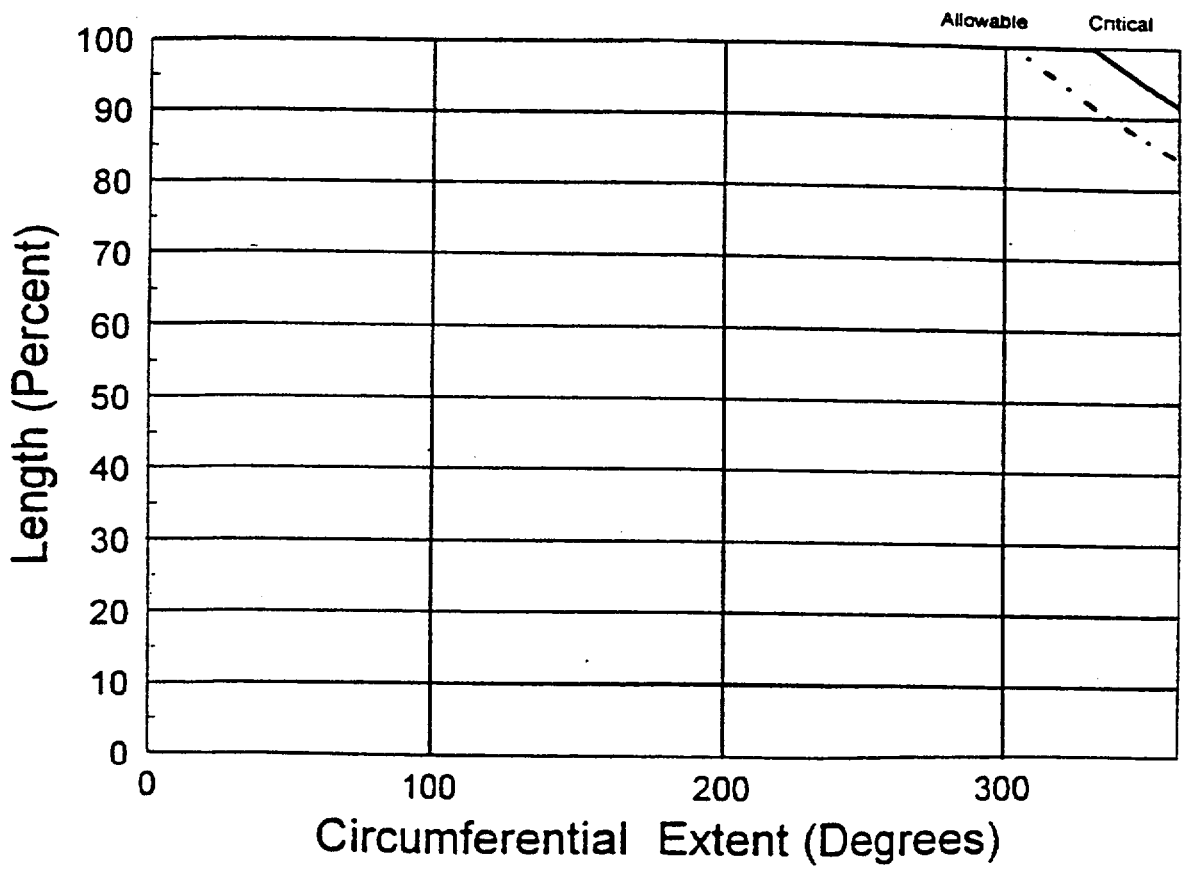

FIGURE A-4

ALLOWABLE REGIONS OF LACK OF FUSION FOR ALL PENETRATIONS:

WELD TO VESSEL FUSION ZONE

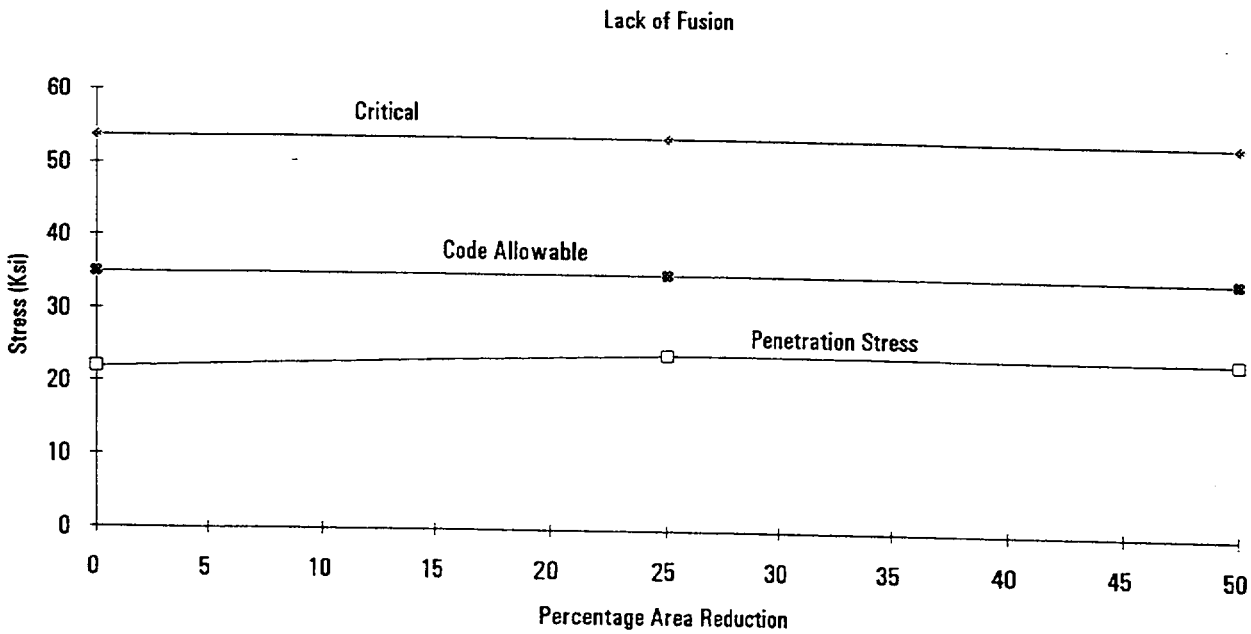

FIGURE A-5

ALLOWABLE REGIONS OF LACK OF FUSION FOR THE WELD TO VESSEL FUSION ZONE

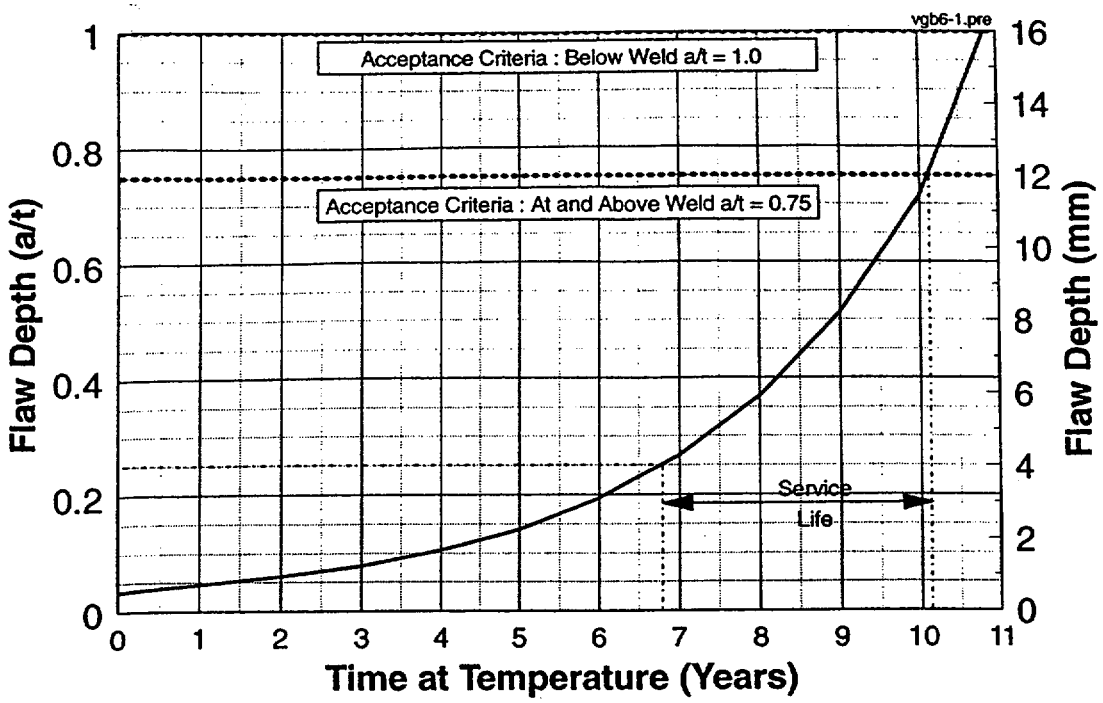

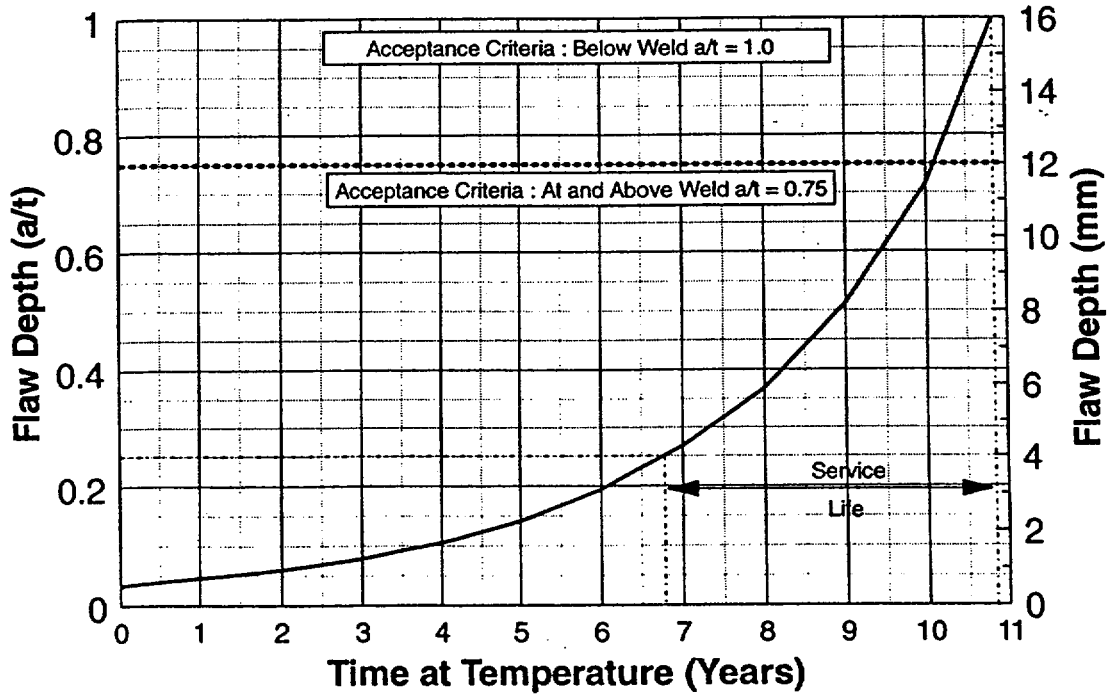

FIGURE B-1

EXAMPLE PROBLEM 1

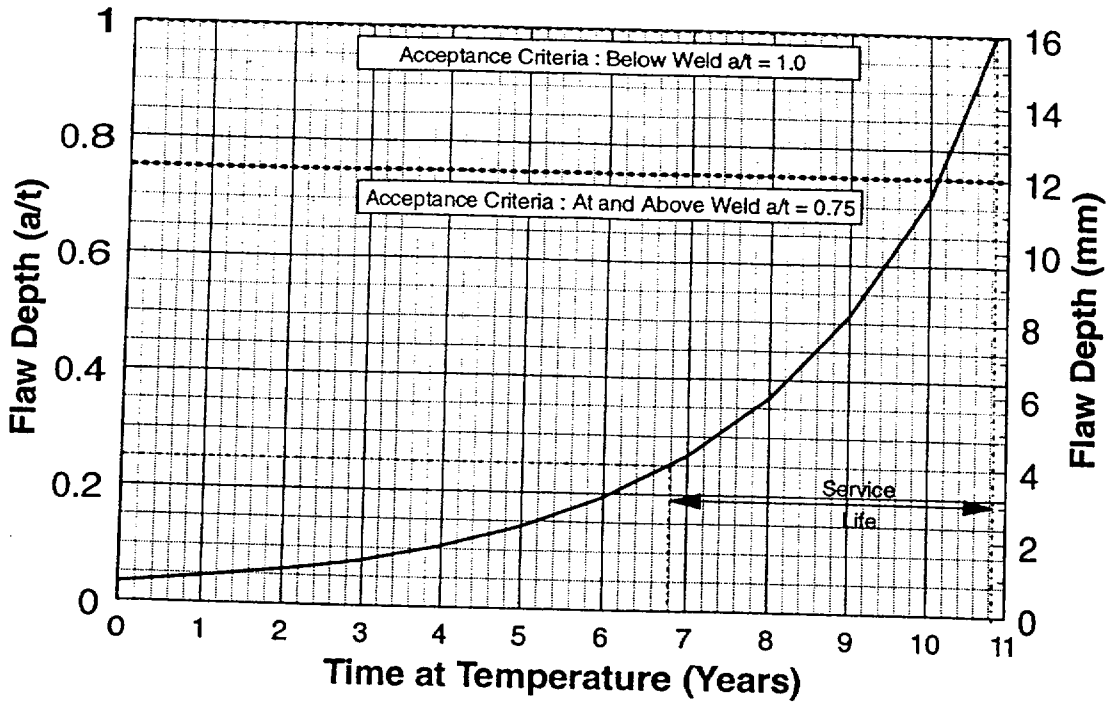

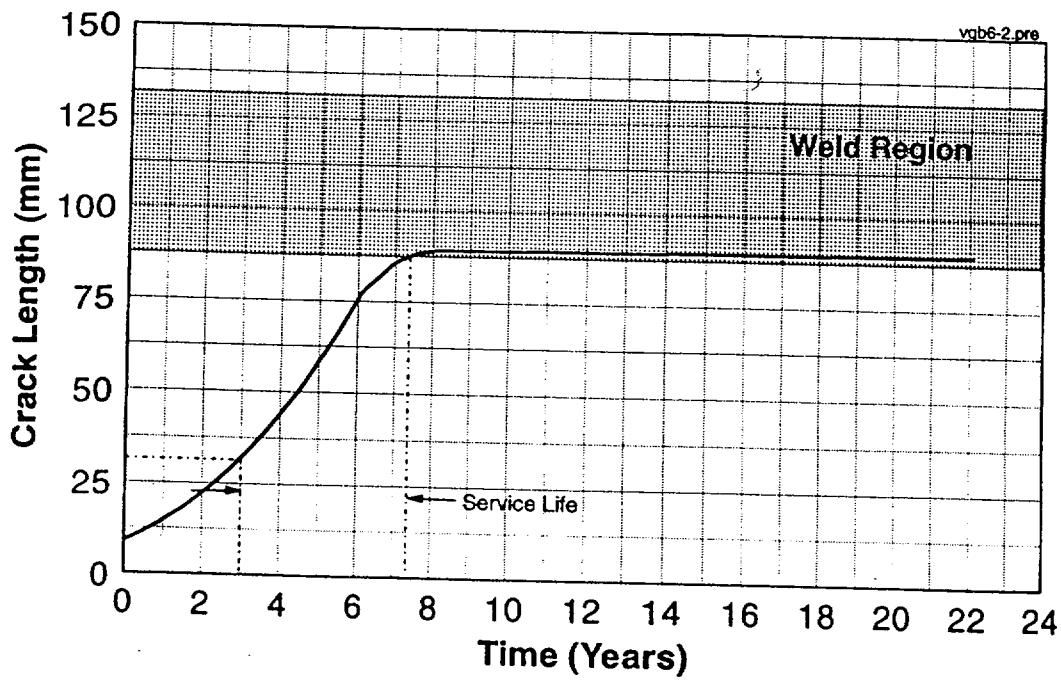

FIGURE B-2

EXAMPLE PROBLEM 2